Translational Oncology 36 (2023) 101753

Contents lists available at ScienceDirect

Translational Oncology

journal homepage: www.elsevier.com/locate/tranon

Original Research

Dissecting the role of lactate metabolism LncRNAs in the progression and immune microenvironment of osteosarcoma

Liangkun Huang [a,†], Xiaoshuang Zeng [a,†], Wanting Liang [b], Junwen Chen [a], Changheng Zhong [a], Wenxiang Cai [a], Xuezhong Wang [a], Zhengjie Zhu [a], Li Su [a], Zilin Liu [a,*], Hao Peng [a,*]

[a] Department of Orthopedics Surgery, Renmin Hospital of Wuhan University, Wuhan Hubei, 430060, China
[b] Department of Clinical Medicine, Xianyue Hospital of Xiamen Medical College, Xiamen, 310058, China

ARTICLE INFO

Keywords:
osteosarcoma
metastasis
lactate metabolism
long non-coding RNA
prognosis
Immune infiltration

ABSTRACT

Background: The process of lactate metabolism has been proved to play a critical role in the progression of various cancers and to influence the immune microenvironment, but its potential role in osteosarcoma remains unclear.
Methods: We have acquired transcriptomic and clinical data from 84 osteosarcoma samples and 70 normal bone samples from the TARGET and GTEx databases. We identified differentially expressed lactate metabolism-related LncRNAs (LRLs) in osteosarcoma and performed Cox regression and LASSO regression to establish LRLs prognostic signature (LRPS). The reliability of LRPS performance was examined by separate prognostic analysis, viability curves and receiver operating characteristic (ROC) curves. Furthermore, the effects of LRPS on the immune microenvironment of osteosarcoma were investigated, and the functions of the focal genes were experimentally validated.
Result: A total of 856 differentially expressed LRLs were identified and 5 of them were selected to construct LRPS, which was a better prognostic predictor for osteosarcoma compared with other published prognostic signatures (AUC up to 0.947 and 0.839 in the training and test groups, respectively, with adj-p<0.05 for KM curves). We found that LRPS significantly affected the immune infiltration of osteosarcoma, while RP11-472M19.2 significantly promoted the metastasis of osteosarcoma, which was well validated experimentally. Encouragingly, a number of sensitive drugs were identified for LRPS and RP11-472M19.2 high-risk groups.
Conclusion: Our study shows that lactate metabolism plays a crucial role in the development of osteosarcoma and has been well validated experimentally, providing extremely important insights into the clinical treatment and in-depth research of osteosarcoma.

Introduction

Osteosarcoma is the most common orthopedic malignancy, often occurs in adolescents [1,2]. Osteosarcoma is easily metastasized to other organs, such as the lungs [3]. The 5-year survival rate of patients with osteosarcoma will be greatly decreased once metastasis occurs [4]. Recently emerging technologies such as neoadjuvant chemotherapy have shown some improvement in the prognosis and survival of patients with osteosarcoma [5,6]. However, poor patient tolerance to chemotherapy and short survival of patients with metastatic osteosarcoma have become very problematic, so it is important to explore the methods to inhibit the metastasis of osteosarcoma and improve the overall survival of osteosarcoma [7,8]. The carcinogenic effect of lactate metabolism on tumors has recently been gradually demonstrated [9]. Lactate is not only a product of glycolysis, but also an important messenger molecule in various pathways [10]. Lactate metabolism has gradually been evidenced as a potential therapeutic target for various tumors [11–13]. A growing number of studies have shown that lactate metabolism plays a non-negligible role in the progression of osteosarcoma [14–19]. Long non-coding RNA (LncRNA) was initially considered as genomic transcriptional "noise" with no biological function, but more and more studies have found that it has important regulatory capabilities in cells [20]. An increasing number of studies have shown that aberrant expression of LncRNAs has a crucial impact on the progression of different tumors [21–27]. Nowadays LncRNA expression levels have been widely used in the diagnosis and prognosis prediction of

* Correspondence:
E-mail addresses: 2019283020147@whu.edu.cn (Z. Liu), penghao0718@163.com (H. Peng).
† These authors contributed equally to this work and share first authorship.

https://doi.org/10.1016/j.tranon.2023.101753
Received 12 June 2023; Received in revised form 15 July 2023; Accepted 1 August 2023

osteosarcoma, for example, Wang et al [28] found that LINC00629 promotes osteosarcoma progression through activation of the KLF4-LAMA4 axis; Yang et al [29] identified six copper death-associated lncRNAs that regulate the immune microenvironment in osteosarcoma and influence survival outcomes in osteosarcoma patients. Notably, recent studies have found that LncRNAs may target lactate metabolism to influence tumor progression [30–32], but the mechanics of the role of LRLs in osteosarcoma are unclear. Therefore, our study focused on finding a new signature of LRLs that can predict the prognosis of osteosarcoma. We integrated TARGET and GTEx databases and constructed a prognostic signature consisting of 5 LncRNAs using COX regression and LASSO analysis, the accuracy of which was well verified, and we also verified the effect of RP11-472M19.2 on osteosarcoma progression experimentally. Our study explores diagnosis, prognosis prediction, and clinical therapy for osteosarcoma from a novel perspective.

Materials and Methods

Access to data

357 lactate metabolism-associated genes were acquired on the gsea website (https://www.gsea-msigdb.org/gsea/index.jsp). Original transcriptomic data and clinical data for OS tissue and normal bone tissue were obtained from the TARGET and GTEx databases (https://xena.ucsc.edu/). The clinical data collected comprised survival status, survival time, metastasis, gender and age. We selected 84 osteosarcoma samples and 70 normal bone tissue having comprehensive clinical data and transcriptomic datasets for further research, and randomly assigned 84 tumor samples into training set (n = 50) and test set (n = 34).

Screening of lactate metabolism-related long noncoding RNAs

We performed Pearson correlation analysis to investigate the correlation between lncRNAs and genes associated to lactate metabolism, both Pearson correlation coefficient (> 0.30) and p value (< 0.001) were used for determining the lncRNAs elating to lactate metabolism.

Identification of Differentially Expressed Gene (DEG)

First, we performed a de-batching process for osteosarcoma samples and human normal samples with the R package "sva". The R package "DESeq2" was then used to identify DEGs among osteosarcoma samples and human normal bone samples, with the test criteria set at fold change = 2 and adjusted P value = 0.05, before being intersected with lactate metabolism-related lncRNAs to obtain differentially expressed lncRNAs associated with lactate metabolism (DELRLs).

Establishing a Prognostic DELRLs Signature

We performed univariate Cox regression on DELRLs based on survival data and transcriptomic data of osteosarcoma samples. The least absolute shrinkage and selection operator (Lasso)-penalized Cox regression was then carried out for obviating overfitting. The optimal and minimum criteria penalized criterion (λ) was determined based on 10 cross-validations. Finally, We used multivariate Cox regression analysis for determining prognostic associated DELRLs as well as constructing LRPS to predict survival of osteosarcoma. Each sample's risk score is determined by the equation: $\boldsymbol{RiskScore} = \sum_{i=1}^{n} \boldsymbol{Coef}_i^* \boldsymbol{X_i}$, while $\boldsymbol{Coef}_i^*$ stands for the coefficients and Xi stands for the normalized expression of the DELRLs. Risk groupings of each sample were determined by the median risk score of all samples.

Predictive power test for LRPS

We adopted Kaplan-Meier (KM) for validating the prognostic predictive ability of LRPS for osteosarcoma. We then utilized receiver operating characteristic (ROC) curves and area under the curve (AUC) for determining the precision of LRPS in predicting osteosarcoma prognosis. We performed principal component analysis (PCA) to verify whether LRPS could significantly differentiate between different risk subgroups for osteosarcoma, and the above results were also visualized with R software packages "rtsne" and "ggplot2". To evaluate the precision of LRPS for outcome prediction, we calculated C-index using R packages "dplyr", "survival", "pec" and "rms". The stability of this signature is verified using test sets and all cohorts.

Exploration of the applicability of LRPS in different clinical characteristics

To verify whether LRPS is stable in osteosarcoma populations with different clinical features, we have investigated the association of LRPS with various clinical features (gender, age, and metastasis) using univariate and multivariate Cox regression assays as a way for investigating the possible impact of these clinical characteristics on osteosarcoma progression.

Exploring DELRLs' ability to predict prognosis of osteosarcoma

The value of different DELRLs in the prognostic prediction of osteosarcoma was analyzed using KM method, and the expression levels of different DELRLs in different risk subgroups were analyzed with box diagram.

Construction of nomogram for LRPS and clinical features

To investigate the capability of LRPS in independently predicting osteosarcoma prognosis, we conducted univariate and multivariate Cox regressions as well as constructed a nomogram using R packages "regplot", "rms" and "survivor". We also built a calibration curve for validating that nomogram's accuracy.

Enrichment analysis of DEGs

We identified DEGs between high- and low-risk groups with R package "DESeq2", and the screening criteria were set as log2 | folding change | > 1 and adjusted P value < 0.05. We utilized R packages "clusterProfiler", "org.Hs.eg.db", "enrichplot" for probing GO and KEGG databases of biologically relevant pathways and analyze in which biologically relevant pathways DEGs are significantly enriched, as a way to probe which biological processes these DEGs may be associated with.

Probing the association between LRPS and the immune microenvironment

We assessed the immune function score and immune cell score of osteosarcoma samples to investigate the potential effect of LRPS on the immune microenvironment of osteosarcoma using the R package "GSVA", and conducted immune checkpoint analysis on these osteosarcoma samples with R package "limma".

Probing potentially sensitive chemotherapy agents

IC50 is an important parameter for obtaining the therapeutic response of tumors, it represents the semi-inhibitory concentration of the measured antagonist and can be used as a criterion to judge the tumor response to drug therapy, the higher the IC50 indicates a lower drug sensitivity and vice versa. We evaluated the response of each osteosarcoma sample to drug therapy to analyze the value of LRPS and individual DELRLs in the clinical management of osteosarcoma using R package "pRRophetic".

Table 1
The primer sequences for qRT-PCR.

Gene	Primer Sequence (5'-3')
GAPDH(F)	GGAAGCTTGTCATCAATGGAAATC
GAPDH(R)	TGATGACCCTTTTGGCTCCC
RP11-472M19.2 (F)	CCTGGGACCCCAGAACCTTA
RP11-472M19.2 (R)	GCAGGTTTCCACCACTCACT

Probing the association between DELRLs and OS metastasis

To investigate whether DELRLs have a potential effect on osteosarcoma metastasis, we explored whether DELRLs expression is different between metastatic subgroups, using box line plots, and performed ROC, AUC, and correlation scatter plots with R packages "ROCR" and "ggplot2", the effect was validated with subsequent experiments.

Exploration of the functionality of a certain DELRL

We apply R package "limma" with pearson correlation coefficient (> 0.30) and p value (< 0.001) to find the most relevant 100 genes for a specific DELRL and enriched these genes in GO and KEGG database pathways for discovering DELRLs' functions.

Cell culture

We purchased the human osteosarcoma cell line SaoS-2 from the American Type Culture Collection (ATCC) and cultured it in Dulbecco's Modified Eagle's medium (DMEM) with 10% fetal bovine serum (FBS), 100 IU/ml penicillin and 100 mg/ml streptomycin, setting the culture conditions at 5% CO2, 37°C.

Gene transfection

RP11-472M19.2-siRNA (RP11-472M19.2 knockdown, denoted as siRNA), the corresponding negative control (denoted as siRNA nc), PCMV-RP11-472M19.2-Neo (RP11-472M19.2 overexpression, denoted as RNAOE), and its negative control (denoted as RNAOE nc) were synthesized by Baiqiandu Biotechnology. Transfection of osteosarcoma cells with siRNAs or plasmids was performed with Lipofectamin 2000 (Invitrogen, USA) according to the instructions. The target sequences of the siRNAs we utilized were: 5'-GCUGCGAGUGAGUGGUGGAAATT-3'.

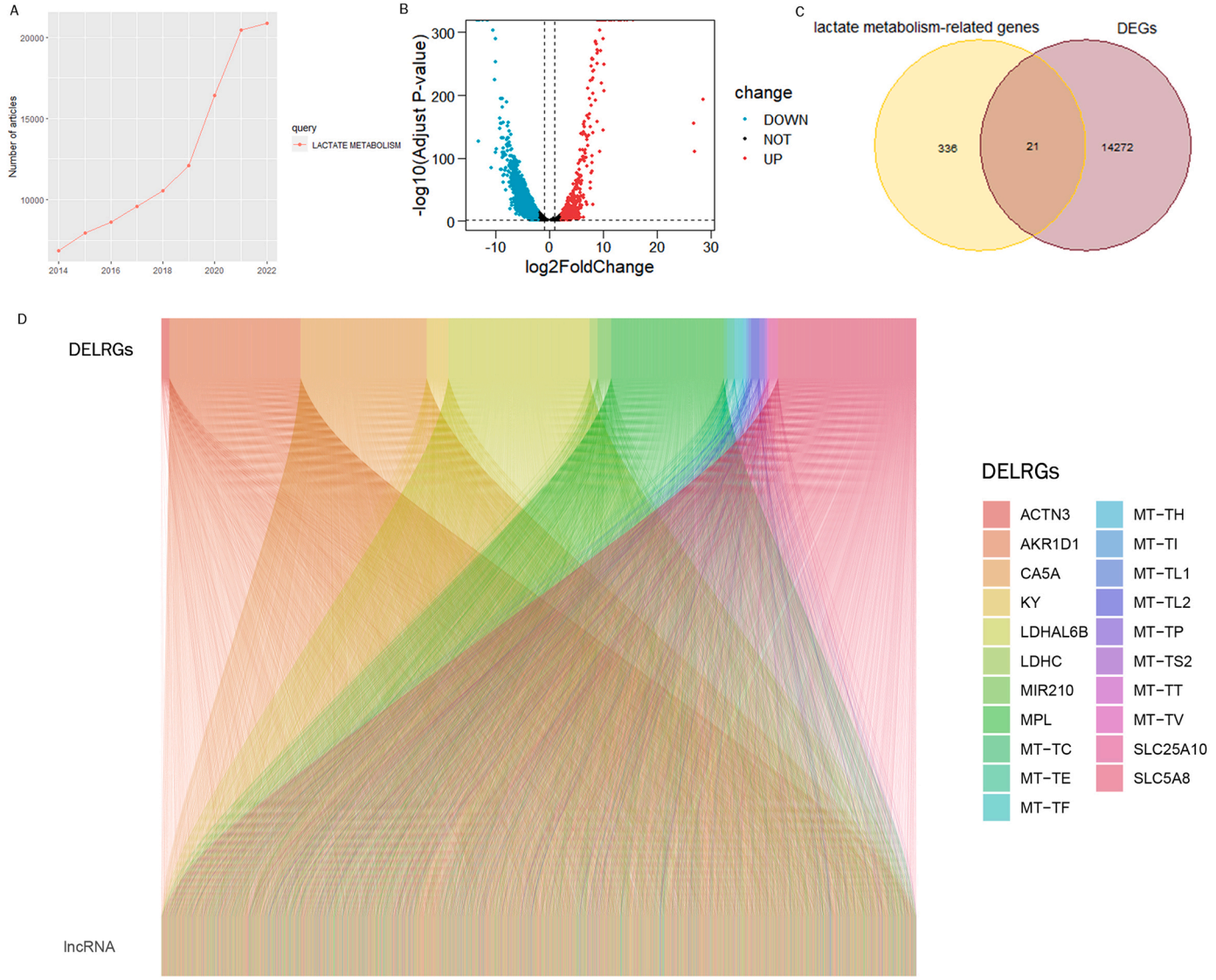

Fig. 1. Acquiring lncrnas related to lactate metabolism. (A) Line graph showing recent research trends in lactate metabolic pathways. (B) Volcano plot showing DEGs between tumor samples and normal samples (screening criteria set to $|\log FC| \geq 2$, padj ≤ 0.05). (C) Venn diagram displaying the intersection of lactate metabolism-related genes and DEGs to obtain 21 DELRGs. (D) Sankey diagram showing the correlation of DELRG and lncRNAs.

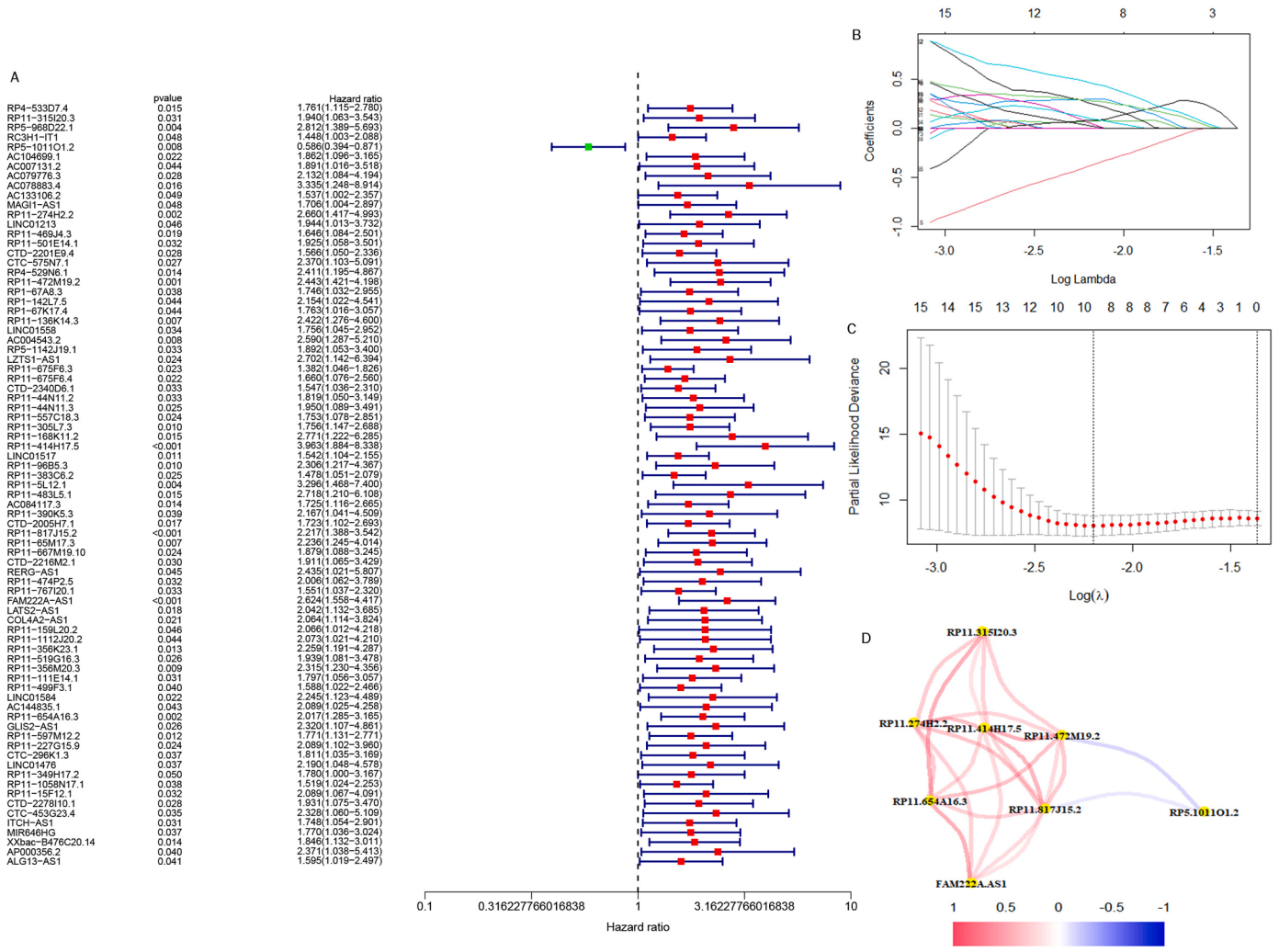

Fig. 2. Acquisition of prognosis-related DELRLs for osteosarcoma. (A) Prognosis-related DELRLs were obtained using univariate Cox regression analysis. (B, C) Lasso-Cox regression analysis of prognosis-related DELRLs. (D) Network diagram of correlation nodes for prognosis-related DELRLs.

Cells without any processing were used as controls (denoted as Control).

Quantitative reverse transcription-PCR (qRT-PCR)

qRT-PCR RNA was extracted from tissue and cells using TRIzol (Invitrogen, Carlsbad, Calif, USA). Then, cDNA was reversely synthesized and transcribed from total RNA using Prime Script RT Reagent Kit (Takara, Dalian, China). Then SYBR Premix Ex Taq II (Takara) was utilized for qRT- PCR analysis. GAPDH was chosen as the internal control. The relative expressions were evaluated by calculating $2^{-\triangle\triangle CT}$ values. The primer sequences see Table 1.

5-Ethynyl-2'-deoxyuridine (EdU) experiment

Cells of different transfection types in logarithmic growth phase were digested with trypsin and configured into cell suspensions and inoculated in 6-well plates in equal volumes. The cells were incubated at 37°C in 5% CO2 incubator for 24h. The cells were washed and fixed with 4% paraformaldehyde for 20min, and the liquid was poured out and washed with PBS buffer. Add EDU reaction solution according to the instructions, then add DAPI to re-stain the nuclei, wash and place under fluorescence microscope to observe and acquire images.

Wound-healing assay

We evenly spread the Saos-2 cells of different transfection types at logarithmic growth stage on 6-well plates after digesting them with trypsin. Place in a 5% CO2, 37°C incubator. When cells reach 90% growth, select a suitable pipette tip and draw straight lines along a sterilized straightedge in the wells. At 0h, 24h and 48h, we photographed and recorded the cells under an inverted microscope and measured their migration distance.

Transwell assay

Saos-2 cells of different transfection types were digested with trypsin and spread evenly on 6-well plates. Place in 5% CO2, 37°C incubator. Cell suspensions containing 2 × 10^4 cells were prepared separately with 200 μL of serum-free medium and added to the upper chamber of transwell. 500 μL of complete medium containing 10% FBS was added to the lower chamber. After 24h of incubation in the incubator, the medium was washed away with PBS and stained with crystal violet for 10 minutes. The surface was washed away with water to remove the crystal violet and photographed under an inverted microscope.

Statistical analysis

We used R software (version 4.2.3) for all statistical analyses. RNA-

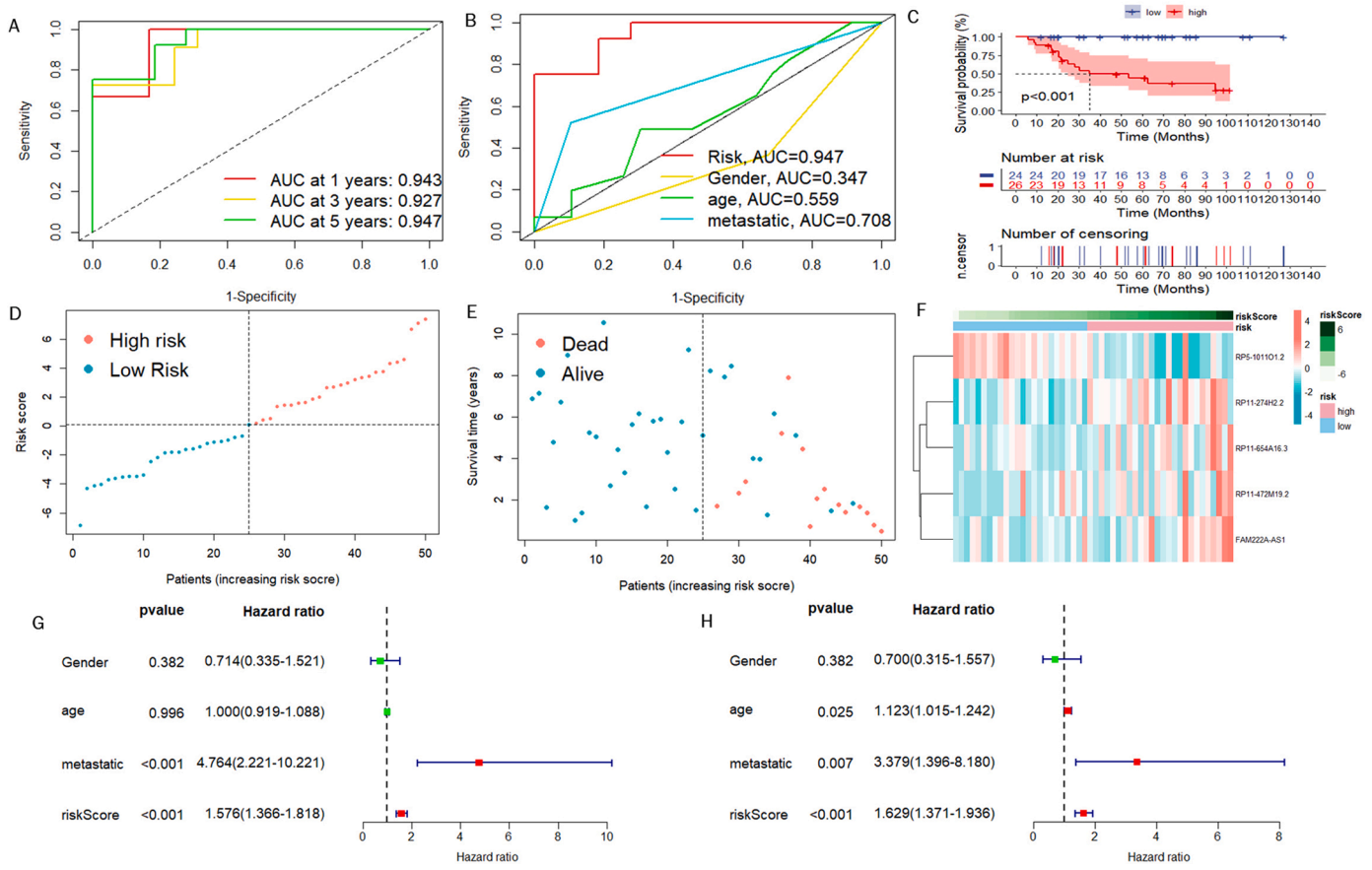

Fig. 3. Evaluation of prognostic predictive power of LRPS. (A) ROC curves for diagnosing patient viability status using LRPS in training group. (B) ROC curves showing that LRPS predicted osteosarcoma prognosis more accurately than all clinical features. (C) Kaplan-Meier curves of LRPS for predicting patients' survival of osteosarcoma in the training set. (D, E) Scatter plots of the viability of osteosarcoma patients in the training set. Green: low risk; Orange: high risk. (F) Heat map showing the expression levels of risk DELRLs in the training set. roc curve, receiver operating characteristic curve; AUC, area under the curve; p<0.05, statistically significant. (G) Univariate Cox analysis for all clinical characteristics and prognostic models. (H) Multivariate Cox analysis.

seq transcriptome data are available from TARGET (https://xena.ucsc.edu/) and the GTEx database (https://xena.ucsc.edu/). Independent t-tests were applied to compare differences in quantitative data across risk subgroups, and correlation of gene expression was calculated by Spearman's correlation coefficient. The criterion for statistical difference was defined as P<0.05.

Results

Screening for lactate metabolism-related lncRNAs

The number of studies on the lactate metabolism pathway showed a significant increase in the last 9 years (Fig. 1A), and we combined the TARGTE and GTEx databases for differential analysis to obtain differentially expressed genes (DEGs) (Fig. 1B), 21 differentially expressed lactate metabolism-related genes (DELRGs) were obtained by crossing with genes associated with lactate metabolism (Fig. 1C). The association of 3264 lactate metabolism-associated LncRNAs with DELRGs was demonstrated in Sankey plots according to Pearson correlation coefficient (set at > 0.30) and p value (set at < 0.001) criteria (Fig. 1D).

LRPS independently predicts prognosis of osteosarcoma

We first obtained 856 DELRLs by taking the intersection of lactate metabolism-related LncRNAs and DEGs, followed by univariate Cox regression analysis and acquired 79 DELRLs associated with osteosarcoma prognosis (Fig. 2A), and then 8 risk DELRLs were identified via LASSO analysis (Fig. 2B and C). According to the correlation network plot (Rcutoff=0.2), RP5-1011O1.2 was found to be negatively correlated with other genes (Fig. 2D). Multivariate Cox analysis was then performed, and we selected 5 DELRLs to create LRPS: RiskScore= 1.62* Expression RP11-274H2.2 + 1.32* Expression RP11-472M19.2 +0.92* Expression FAM222A-AS1+ 0.64* Expression RP11-654A16.3 -1.51* Expression RP5-1011O1.2. We then placed all osteosarcoma samples into different risk subgroups according to their median risk scores. Univariate and multivariate Cox regression analyses were conducted for verifying the ability of LRPS to independently predict osteosarcoma prognosis. It was revealed that both risk scores and metastasis were statistically significant (Fig. 3G). Also, multivariate Cox regression shows that they still reside to be significant, indicating that they can independently predict the prognosis of osteosarcoma (Fig. 3H). ROC curves, risk curves, heat maps and Kaplan-Meier survival curves in Fig. 3A-F revealed that LRPS provides an accurate diagnosis of osteosarcoma prognosis with AUCs as high as 0.943, 0.927 and 0.947, at 1, 3 and 5 years, correspondingly (Fig. 3A-F). The higher AUC values of LRPS than other clinical features suggest that LRPS is a stronger predictor of prognosis in osteosarcoma. We further explored the prognostic value of LRPS according to different clinical characteristics, we grouped osteosarcoma samples according to gender, age (<14 and ≥14 years) and metastatic status separately and plotted KM survival curves, the results in Fig. 4 demonstrate that there are also significant differences in survival rates among different clinical subgroups, all the above results suggest that LRPS in different clinical subgroups can predict the prognosis of osteosarcoma stably and it could be a valuable independent

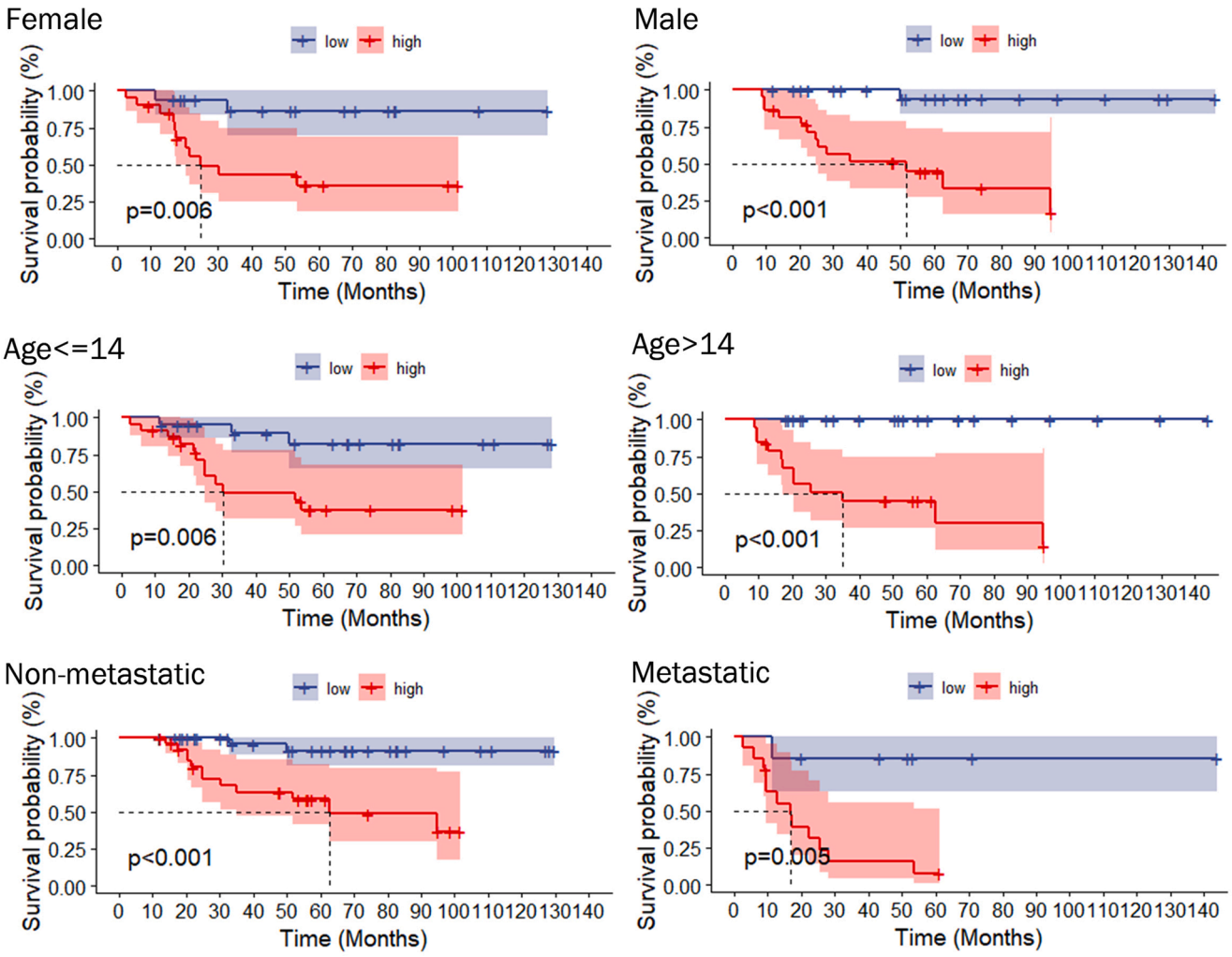

Fig. 4. Kaplan-Meier analysis after subgrouping by different clinical traits (age, sex, and metastasis).

prognostic factor.

Validation of LRPS

To assess the stability of LRPS, we carried out the identical analyses for test group and all cohorts. Fig. 5A and B show that AUC values reached 0.737, 0.846, and 0.839 at 1, 3, and 5 years in test set, respectively, while AUC values for all cohorts reached 0.836, 0.882, and 0.880, too. AUC values for LRPS and other clinical features were measured in the test set and in all cohorts, and still showed a stable prognostic value of LRPS for osteosarcoma (Fig. 5C and D). As well, KM survival curves for test group and all cohorts verified that LRPS can be a promising predictor of osteosarcoma survival prognosis (Fig. 5E and F). This was also validated by risk curves and heat maps (Fig. 5G-L). We performed PCA to probe the degree of differentiation between different risk subgroups. The results in Fig. 6A-C have revealed that LRPS performed well in distinguishing different risk subgroups, while the division based on 856 DELRLs and all genes did not distinguish separate risk subgroups to two clusters.

Separate Validation of DELRLs for Prognostic Prediction of Osteosarcoma

The box plot in Fig. 6D shows that the expression of RP5-1011O1.2 was significantly higher in the low-risk group, while the expression of RP11-274H2.2,RP11-472M19.2,FAM222A-AS1 and RP11-654A16.3 was significantly lower (Fig. 6E-H). KM curves show that expression of RP5-1011O1.2, RP11-274H2.2 and RP11-472M19.2 can all predict the osteosarcoma prognosis individually (Fig. 6I-M).

Nomogram construction and validation

We constructed a nomogram for predicting the viability of osteosarcoma patients at different time points in Fig. 7A. As shown in Fig. 7B, the calibration curves confirm a satisfactory match between the predicted results of the nomogram and actual survival of patients with osteosarcoma. As seen in Fig. 7C, the C-index confirms that LRPS can predict osteosarcoma prognosis more accurately than other clinical characteristics. We have constructed a ROC curve according to the nomogram and calculated an AUC value up to 0.868 (Fig. 7D), confirming that the nomogram can predict osteosarcoma prognosis with high efficiency.

Biological pathway enrichment analysis for different risk subgroups

We obtained 419 DEGs with significantly elevated gene expression levels in the high-risk group by differential expression analysis, and conducted GO and KEGG enrichment analysis with these genes. Among the categories of biological process, these genes were mainly enriched in response to oxygen levels, muscle system processes, and regulation of ion transmembrane transporter activity. Among the categories of cellular formation, the main enrichments were identified in neuronal cell body, contractile fiber, etc. Among the categories of molecular

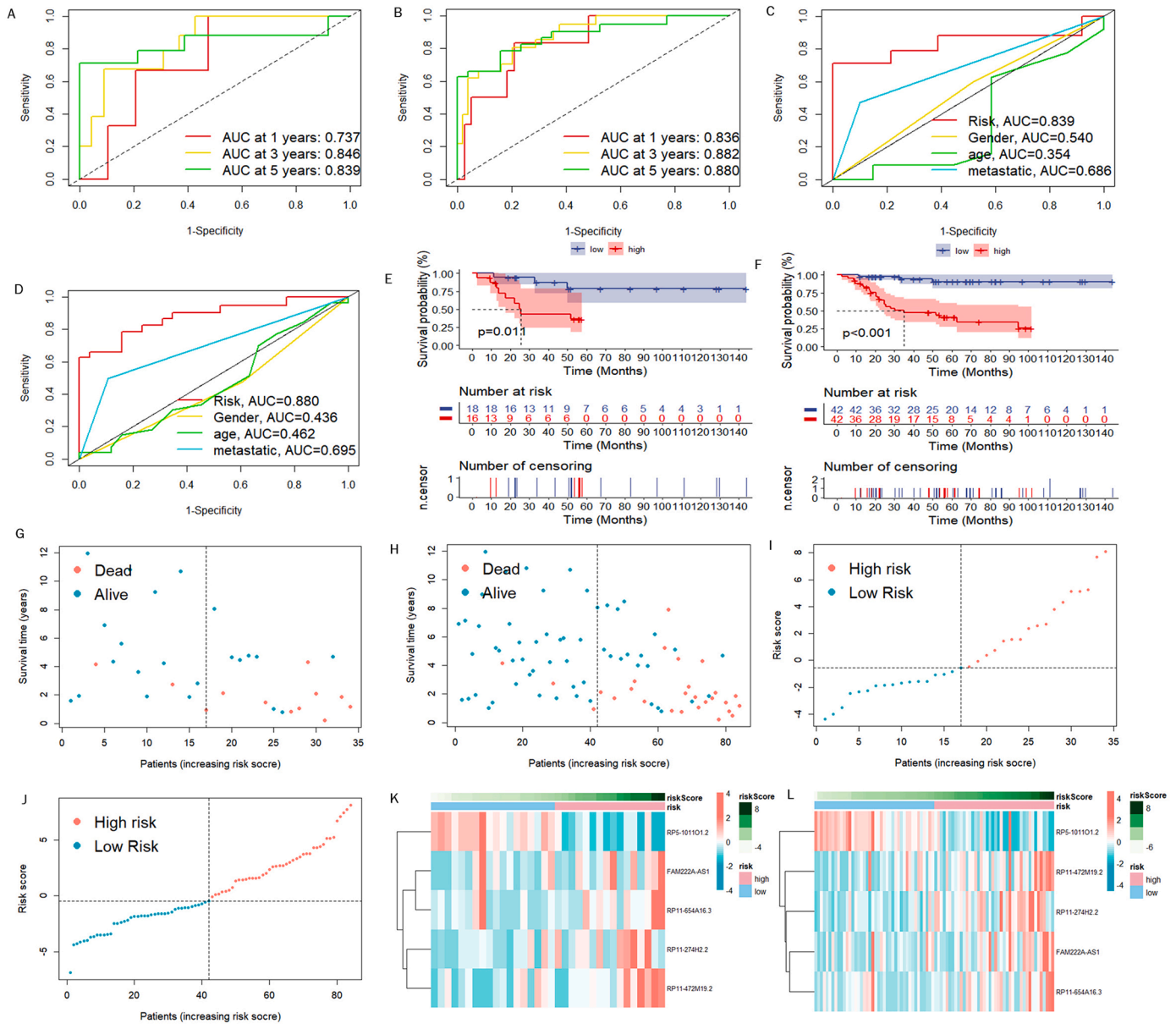

Fig. 5. Examination of LRPS in test group and entire cohort. ROC curves for LRPS diagnosing osteosarcoma survival status in the test group (A) and entire cohort (B). the ROC curves show that LRPS is more accurate than other clinical features in diagnosing osteosarcoma survival status in the test set (C) and the whole cohort (D). Kaplan-Meier curves for overall survival were plotted with the test group (E) and the entire cohort (F). Point plots of patients' viability in the test group (G, I) and in the whole cohort (H, J). Green: low risk; Orange: high risk. Heat map showing risk DELRLs' expression levels in test group (K) and whole cohort (L).

function, the main enrichments were identified in actin binding, receptor activity and G protein-coupled receptor binding (Fig. 8A, C, E). the KEGG enrichment analysis revealed that these genes primarily enriched in human papillomavirus infection, neuroactive ligand-receptor interaction, etc. (Fig. 8B, D and F).

Exploring the potential impact of LRPS on the immune microenvironment

To investigate the possible effects of LRPS on the status of immunological microenvironment in osteosarcoma, multiple immune assessment algorithms were performed. As shown in Fig. 9A, compared to the low-risk group, patients in the high-risk group had lower immune, ESTIMATE scores and higher tumor purity. Fig. 9B shows a significant downregulation of B cells, CD8+ T cells and DCs in the high-risk group, and these patients had lower T cell co-stimulation scores (Fig. 9C). In addition, Fig. 9D shows higher levels of CD160 and ICOSLG expression in the high-risk group, suggesting that LRPS has a potential effect on the immune checkpoint-associated genes expression. Fig. 9E shows that patients in the low-risk group have a higher degree of immune infiltration. Fig. 10 shows a significant correlation of risk scores and risk subgroups with immune cells, immune function and immune checkpoints. All these results demonstrate the powerful effect of LRPS on the Immunological microenvironment of osteosarcoma which can reveal the immune status of osteosarcoma patients to a certain extent.

Exploration of potential chemotherapeutic agents

Targeted drug therapy has become a valuable tool in current oncology treatment. We explored the effect of LRPS on the IC50 of osteosarcoma therapeutic agents to explore the value of LRPS in osteosarcoma treatment. We compared the differences in IC50 of different anti-cancer drugs in distinct risk subgroups. Fig. 11 shows that the IC50 of BMS345541 and JNK-9L were statistically lower in the high-risk group identified by LRPS (set as $P<0.001$), suggesting that patients of

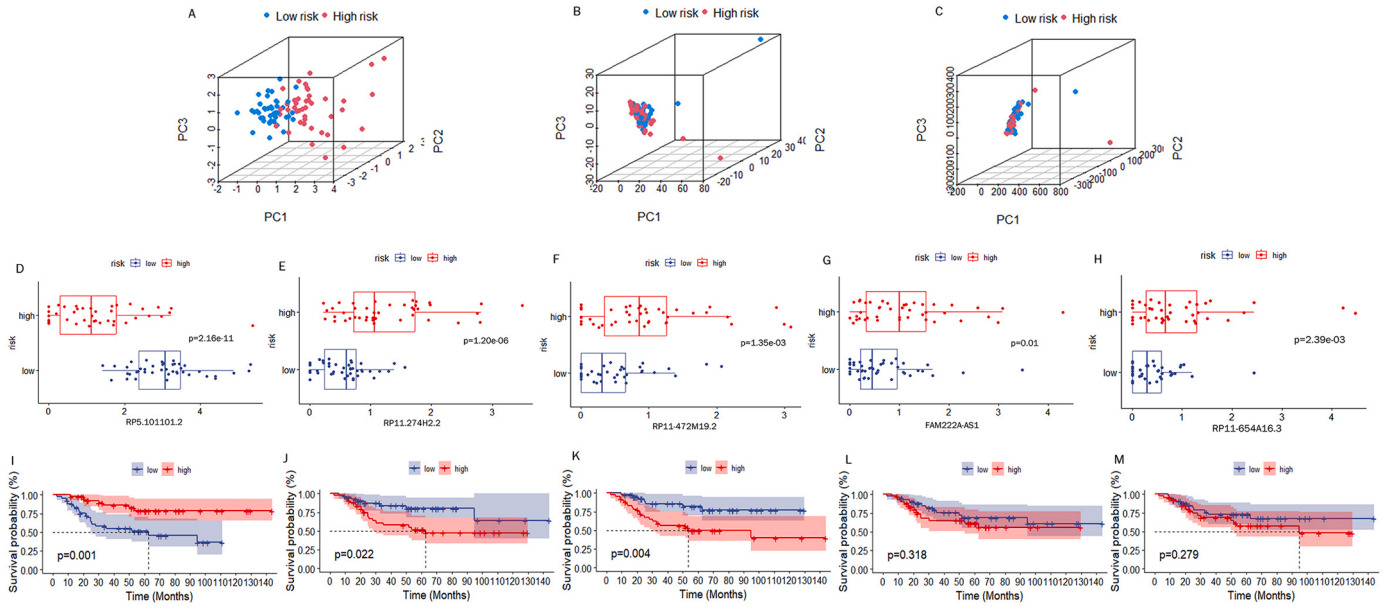

Fig. 6. Independent analysis of the prognostic predictive power of DELRLs. PCA plots demonstrate the ability of LRPS (A), 856DELRLs (B) and all genes (C) to cohort all samples. Box plots demonstrate the differential expression of risk DELRLs in different risk subgroups (D-H). Kaplan-Meier curves show the potential of each DELRLs for predicting survival in osteosarcoma (I-M).

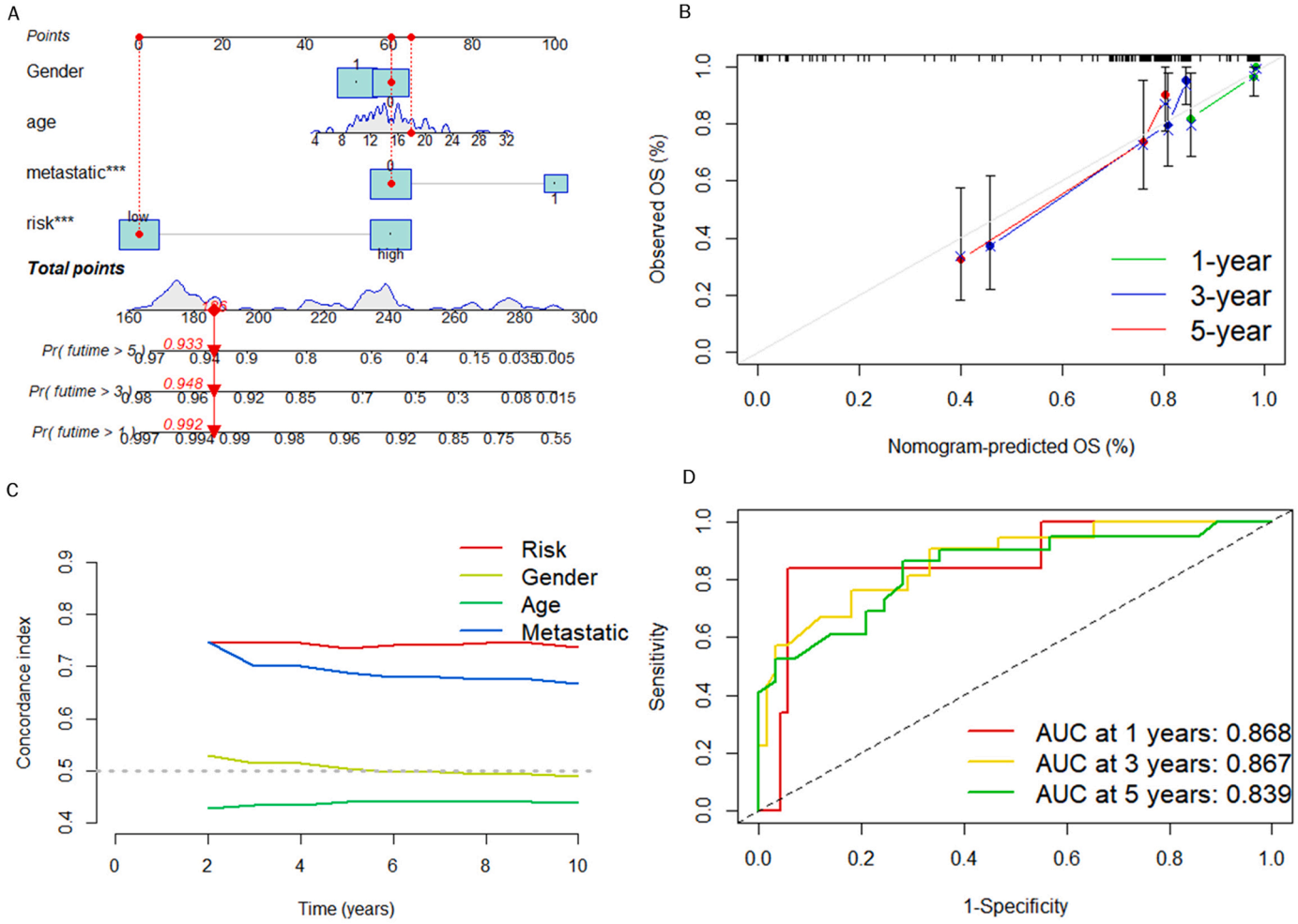

Fig. 7. LRPS-based nomogram was constructed and validated with the entire cohort. (A) Construction of a nomogram based on LRPS. (B) Calibration curve was performed to verify the reliability of nomogram. (C) C-index curves for evaluating the forecasting ability of LRPS and other clinical characteristics at different time points. (D) ROC curves of nomogram for diagnosing osteosarcoma survival status.

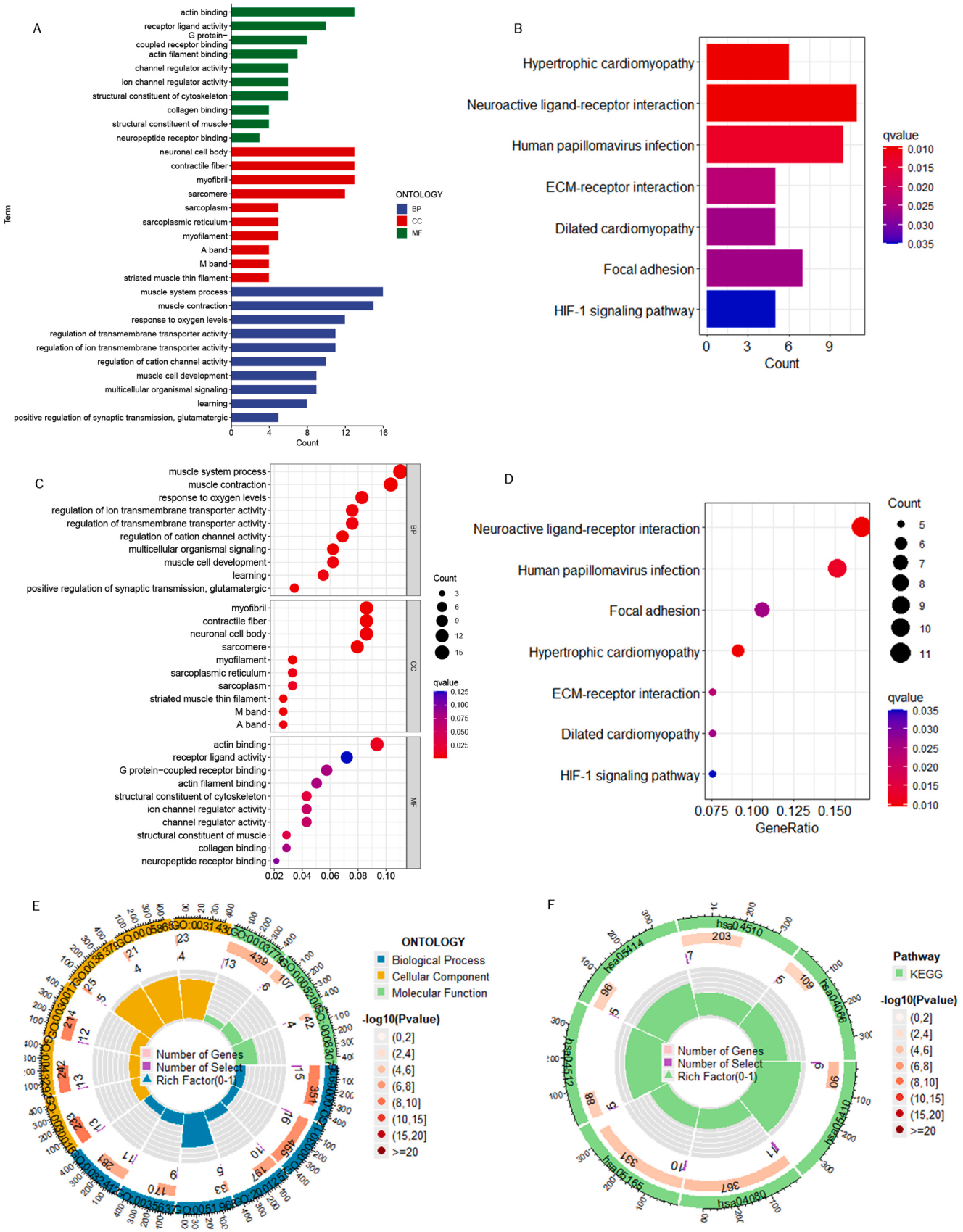

Fig. 8. Pathway enrichment analysis of GO and KEGG. (A) Histograms of the top 10 GO-enriched terms. (B) Histograms of the top 7 KEGG-enriched terms. (C) A bubble plot of the top 10 GO-enriched terms. (D) A bubble plot of the top 7 KEGG-enriched terms. (E) Circle plot of GO enrichment analysis. (F) Circle plot of KEGG enrichment analysis.

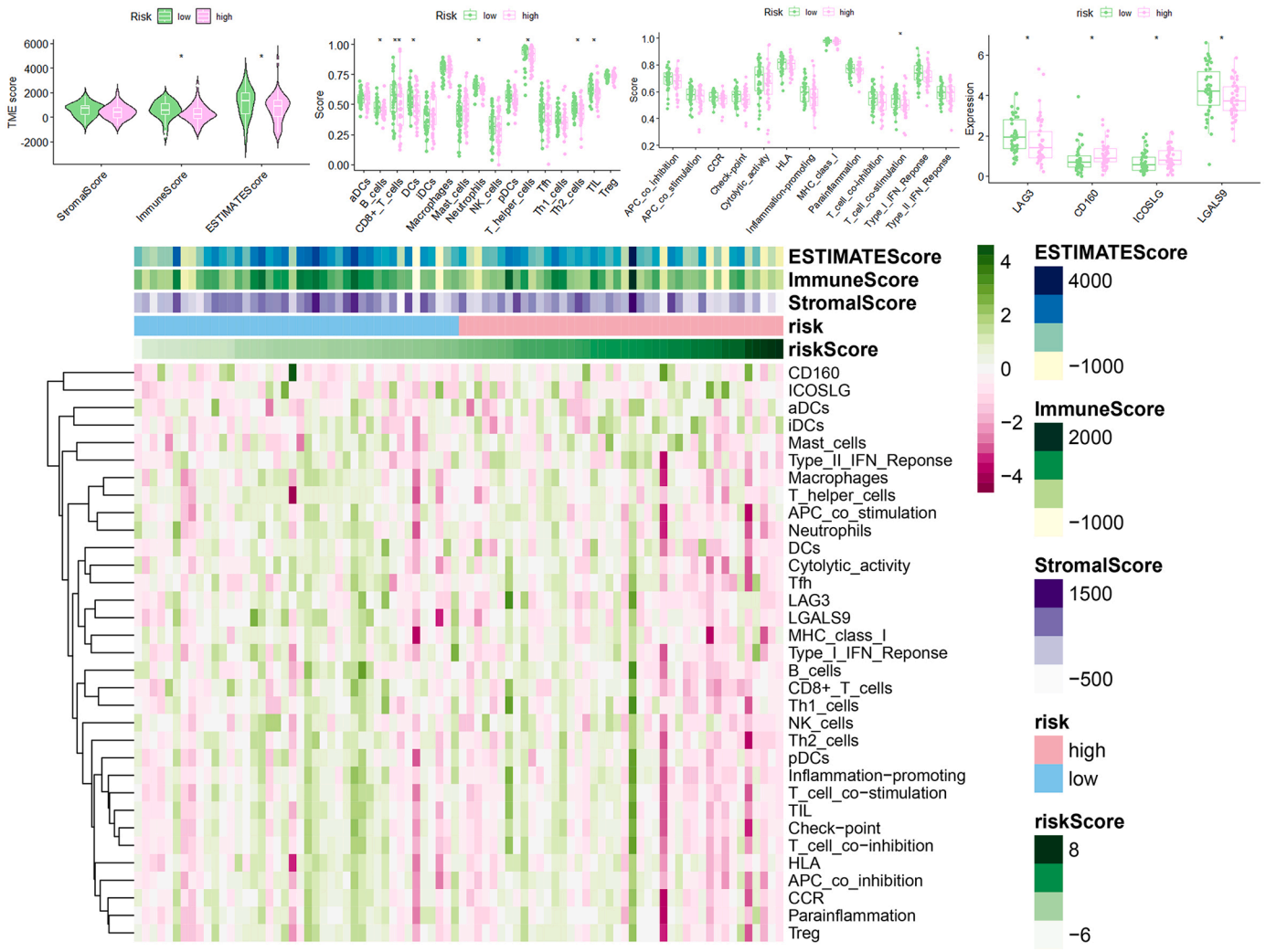

Fig. 9. Immunoassays demonstrated that LRPS significantly influenced the immune microenvironment of osteosarcoma. (A) TME of osteosarcoma was significantly different among different risk subgroups. The 7 immune cells (B), 1 immune-related function (C) and 4 immune checkpoints (D) had significant differences in scores between two risk subgroups. (E) Immunological heat map shows that there are significant differences in immunological characteristics between the two risk subgroups.

high-risk group have better susceptibility to those two agents.

Exploring the relationship between RP11-472M19.2 and osteosarcoma metastasis

Plotting ROC curves for all cohorts for the 5 DELRLs and calculating AUC values (Fig. 12A-E) showed that only RP11-472M19.2 expression was valid for predicting osteosarcoma metastasis (Fig. 12E), with equally satisfactory results for the training set (Fig. 12G). The box plot shows that RP11-472M19.2 is significantly differentially expressed in different metastatic subgroups of osteosarcoma (Fig. 12F). Furthermore, Fig. 12H shows the correlation between the expression of RP11-472M19.2 and genes associated with osteosarcoma metastasis. RP11-472M19.2 was positively correlated with genes involved in promoting osteosarcoma metastasis such as MET, FASN, HES4, EZH2, DNMT3A and HEY1, and negatively correlated with genes inhibiting osteosarcoma metastasis such as FAS and DCN. suggesting that the effect of RP11- 472M19.2 expression level on osteosarcoma metastasis is not negligible.

Exploration of the potential functions and roles of RP11-472M19.2

We obtained 100 genes most positively or negatively associated with RP11-472M19.2 to make an expression heat map (Fig. 13A), showing that high expression of RP11-472M19.2 was associated with more osteosarcoma metastases. Enrichment analysis of these genes showed that they were involved in integrin binding, extracellular matrix binding, external encapsulating structure organization, cell substrate adhesion. response to amino acid, cellular response to acid chemical, response to hyperoxia and other GO pathways (Fig. 13B), and in the KEGG pathway including protein digestion and absorption. proteoglycans in cancer, and relaxin signaling pathway (Fig. 13C). According to RP11-472M19.2 expression level, two subgroups were divided and differential analysis was performed, and the differential genes were obtained as shown in Fig. 13D, which showed that these differential genes were significantly enriched in acidic amino acid transport, amino acid transport, carboxylic acid transport, cell-cell contact zone, skeletal muscle organ development and other pathways (Fig. 13E). Chemotherapy agents sensitivity analysis for different risk subgroups based on RP11-472M19.2 reveals that the IC50 values of drugs BMS345541, KIN001-135, LAQ824, Pyrimethamine, QS11, Salubrinal, Thapsigargin, CP724714, MP470, Vorinostat and VX-702 were lower in the high-risk group (Fig. 14), suggesting their greater sensitivity toward these drugs.

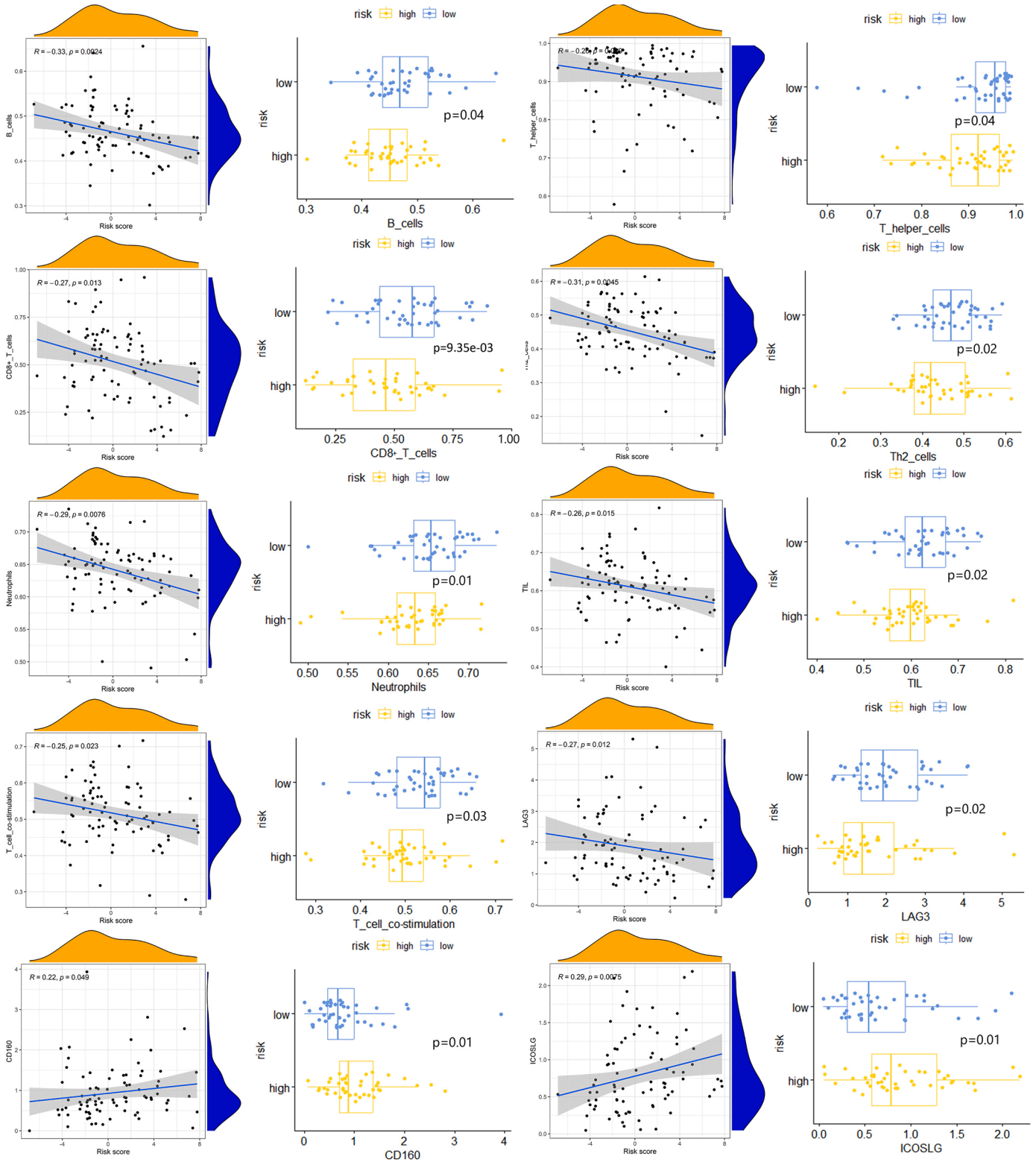

Fig. 10. shows the correlation of immune function, immune cells and immune checkpoints with risk scores, as well as immune correlation scores between two risk subgroups.

RP11-472M19.2 promotes osteosarcoma progression

The pcr results in Fig. 15 showed that the expression level of RP11-472M19.2 was notably decreased in siRNA group comparing to the control and siRNA nc groups, and it was remarkably up-regulated in the RNAOE group comparing to the control group and RNAOE nc group. This indicates that we successfully knocked down or overexpressed RP11-472M19.2 in SaoS-2 cells. EdU assays were performed on different transfection types of Saos-2 cells to detect their proliferation. Fig. 16 shows that RP11-472M19.2 has a proliferative effect on the proliferation of osteosarcoma cells. Wound healing assays were performed on different transfected types of Saos-2 cells to examine their migratory

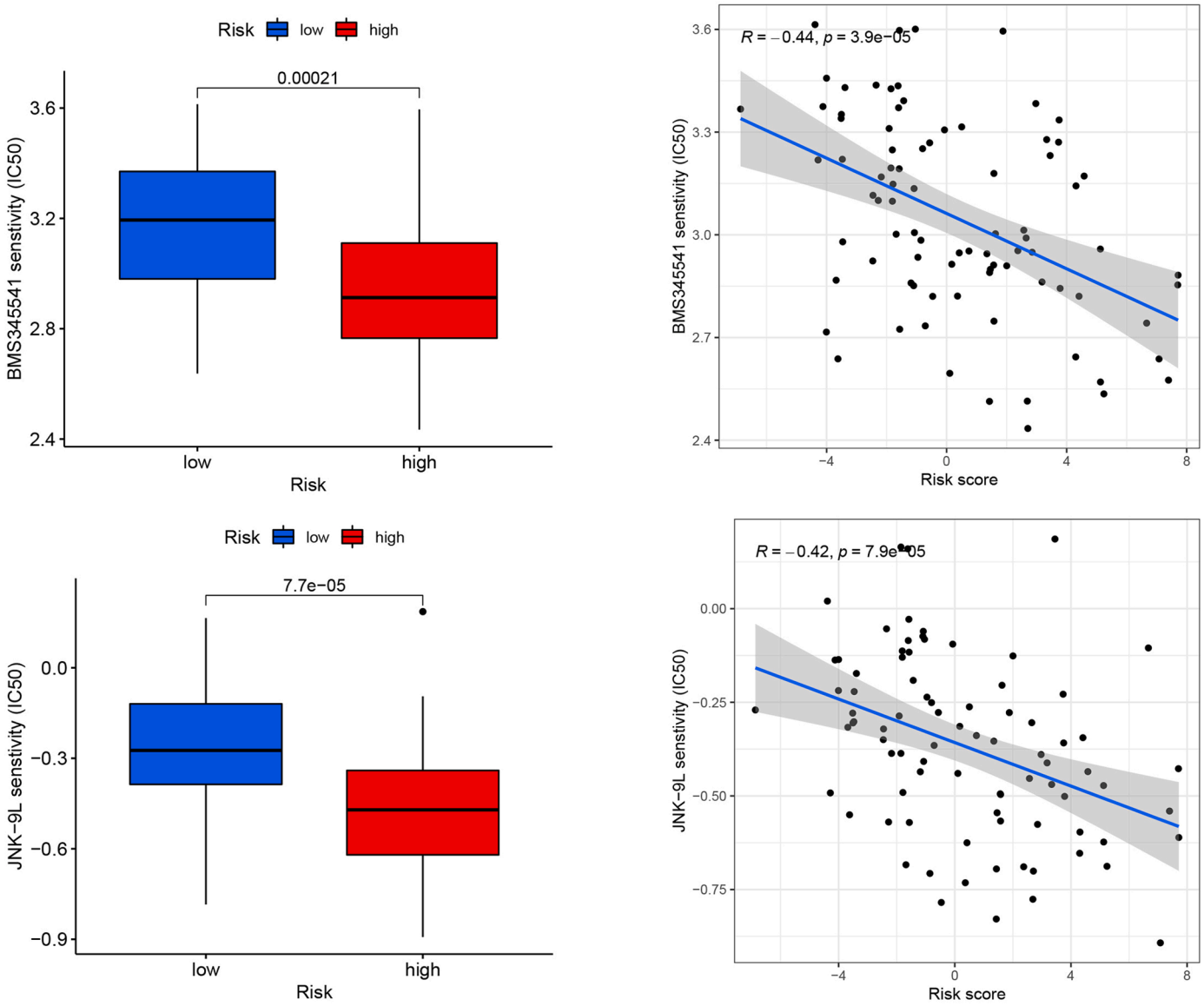

Fig. 11. Chemotherapy agent sensitivity analysis shows that the IC50 of BMS345541 and JNK-9L were statistically lower in the high-risk group identified by LRPS.

ability, and Fig. 17 shows that RP11-472M19.2 has a promotive effect on the migrating ability of Saos-2 cells. Fig. 18 shows that overexpression of RP11-472M19.2 had a promoting effect on Saos-2 cell invasion, whereas knockdown had an inhibitory effect, suggesting that RP11-472M19.2 could enhance the invasion ability of Saos-2 cells. All these results confirm that RP11-472M19.2 can influence the evolution and metastasis of osteosarcoma.

Discussion

As a prevalent malignancy in adolescents, osteosarcoma is gradually considered a major public health and economic threat because of its poor prognosis and susceptibility to recurrence and metastasis to other organs such as lungs [1]. And since the Warburg effect was proposed [9], the role of lactate metabolism in various tumors has gradually gained attention and the number of related studies has increased greatly. Recent studies on lactate metabolism in osteosarcoma have also been increasing [14–19]. LncRNAs can regulate gene expression at multiple levels (e.g. epigenetic regulation and transcriptional regulation), they are increasingly being studied as biomarkers for various cancers [33–37]. But to our knowledge, there are few studies combining lactate metabolism-related lncrnas and osteosarcoma, so we focused on the interconnection of lncRNA and lactate metabolism in osteosarcoma to explore the value of lactate metabolism-related lncrnas in prognosis prediction and treatment guidance for osteosarcoma.

We combined the TARGET and GTEx databases and used Pearson correlation analysis (coefficient set to >0.3, p value set to <0.001) to create a prognostic predictive signature for osteosarcoma comprising five lactate metabolism-associated lncRNAs for the first time based on the experience of previous scholars studying related lncRNAs [38–41]. In the correlation node network graph of the eight DELRLs, RP5-1011O1.2 was negatively correlated with other genes, while all other genes were positively correlated with each other, indicating that RP5-1011O1.2 may be a security gene for patients with osteosarcoma. To assess the predictive power of the prognostic model, we classified each sample into different risk subgroups according to the median risk score of all osteosarcoma samples and carried out ROC, risk heat map, and KM analyses, which yielded good results in both the training and test sets, The 1-, 3-, and 5-year AUC values for LRPS predicting osteosarcoma survival in the test set reached 0.836, 0.882, and 0.880, and multivariate cox analysis revealed that LRPS could independently predict the prognosis of patients with osteosarcoma. All samples were

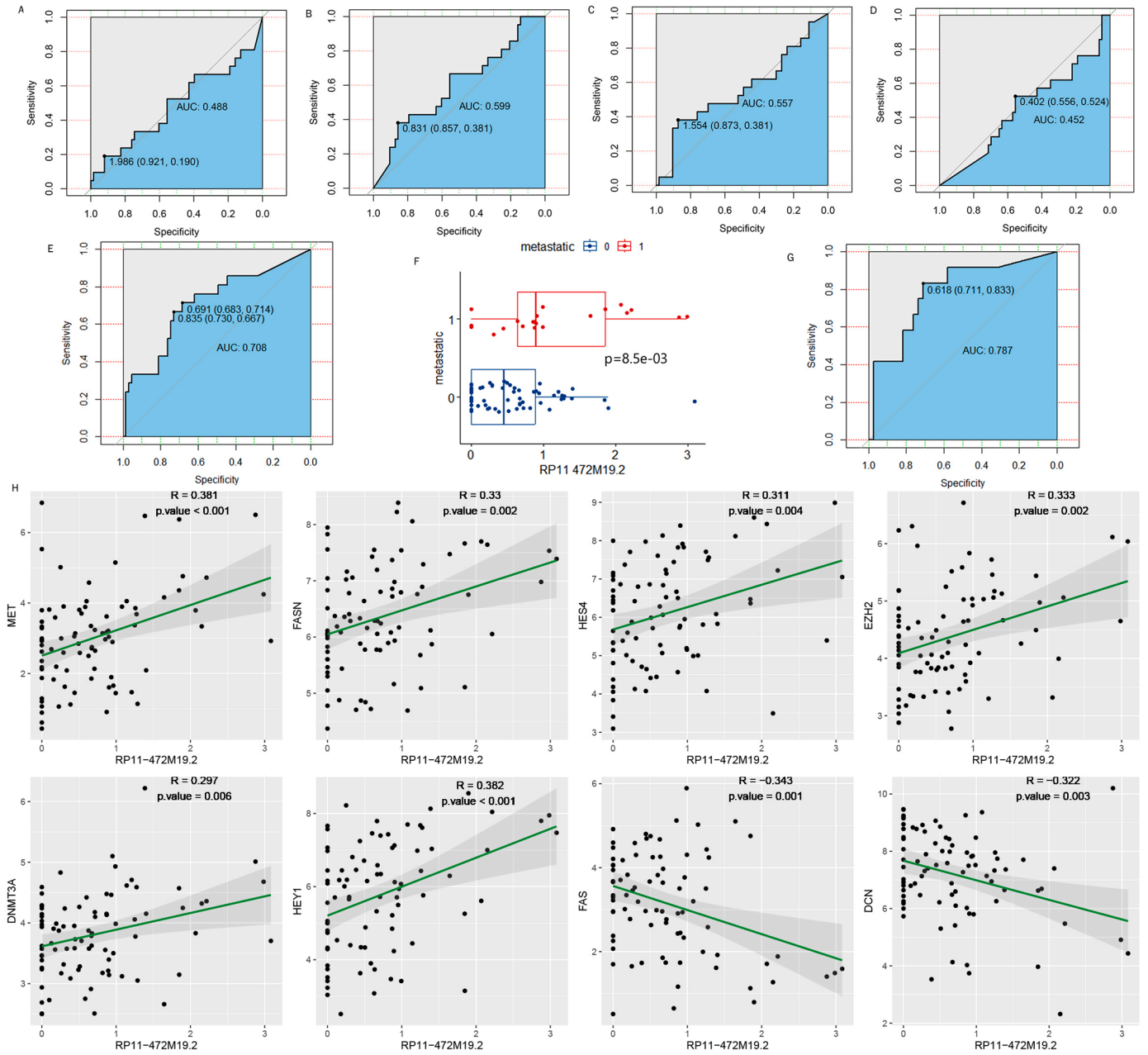

Fig. 12. To explore the relationship between osteosarcoma metastasis and RP11-472M19.2. ROC curves for predicting osteosarcoma metastasis in the whole cohort of FAM222A-AS1, RP5-1011O1.2, RP11-274H2.2, RP11-654A16.3. RP11-472M19.2 was used in the whole cohort (E) and training group (G) for diagnosing osteosarcoma metastasis. (F) Box plot showing significantly higher expression of RP11-472M19.2 in the metastasis group. (H) Dot plot of the correlation between osteosarcoma metastasis-associated gene MET, FASN, HES4, EZH2, DNMT3A, HEY1, FAS, DCN expression and the expression of RP11-472M19.2.

grouped by clinical features including age, sex and whether they metastasized and tested the stability of LRPS. The results demonstrated that LRPS performed stably in all clinical subgroups, demonstrating the good applicability of LRPS. And PCA analysis indicated that LRPS can well separate the different risk subgroups into two clusters. All five DELRLs we screened showed significantly different expression in different risk subgroups, and KM curve analysis of RP5-1011O1.2, RP11-274H2.2, and RP11-472M19.2 showed that they all can independently predict viability in osteosarcoma patients, demonstrating the strong potential of these five DELRLs for prognostic prediction of osteosarcoma. We have constructed a nomogram to forecast the prognosis of osteosarcoma, and the calibration curve and C-index indicate a high consistency between the predicted results of the nomogram and the actual, and ROC curve revealed a good forecasting capability of this nomogram for osteosarcoma patients. Enrichment analysis based on DEGs between different risk subgroups showed that they were mainly enriched in pathways neuroactive ligand-receptor interaction, HIF-1 signaling, receptor ligand activity, and G protein-coupled receptor binding, suggesting that lactate metabolism may have an impact on OS progression through these complex pathways, which can be further explored in the future.

We explored the ability of five key lncRNAs to predict osteosarcoma metastasis and found that only RP11-472M19.2 had excellent performance in predicting osteosarcoma metastasis. Boxplot and ROC curves demonstrate that RP11-472M19.2 may be a potential predictor of osteosarcoma metastasis. The expression level of RP11-472M19.2 was significantly higher in the metastatic group of osteosarcoma compared to the non-metastatic group, AUC values for predicting osteosarcoma

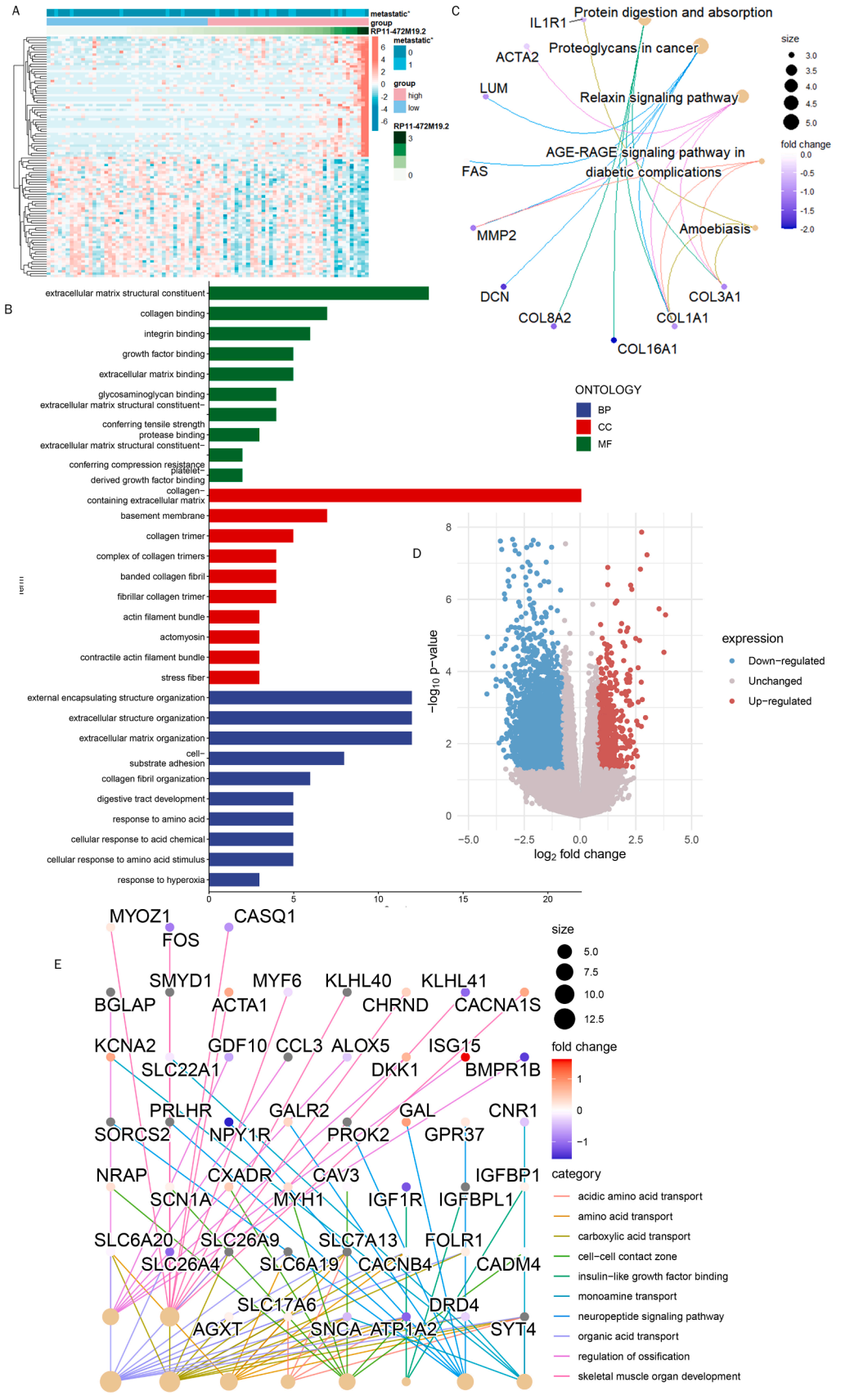

Fig. 13. Investigation of the pathways involved in RP11-472M19.2. (A) Gene expression heat map displaying the 50 genes those have strongest positive or negative associations with RP11-472M19.2. (B, C) The 100 genes with the strongest association with RP11-472M19.2 were analyzed for enrichment in biologically relevant pathways. (D) Volcano plot showing differentially expressed genes screened in two subgroups based on RP11-472M19.2 expression levels. (E) Results of the enrichment analysis based on the differentially expressed genes screened in figure D.

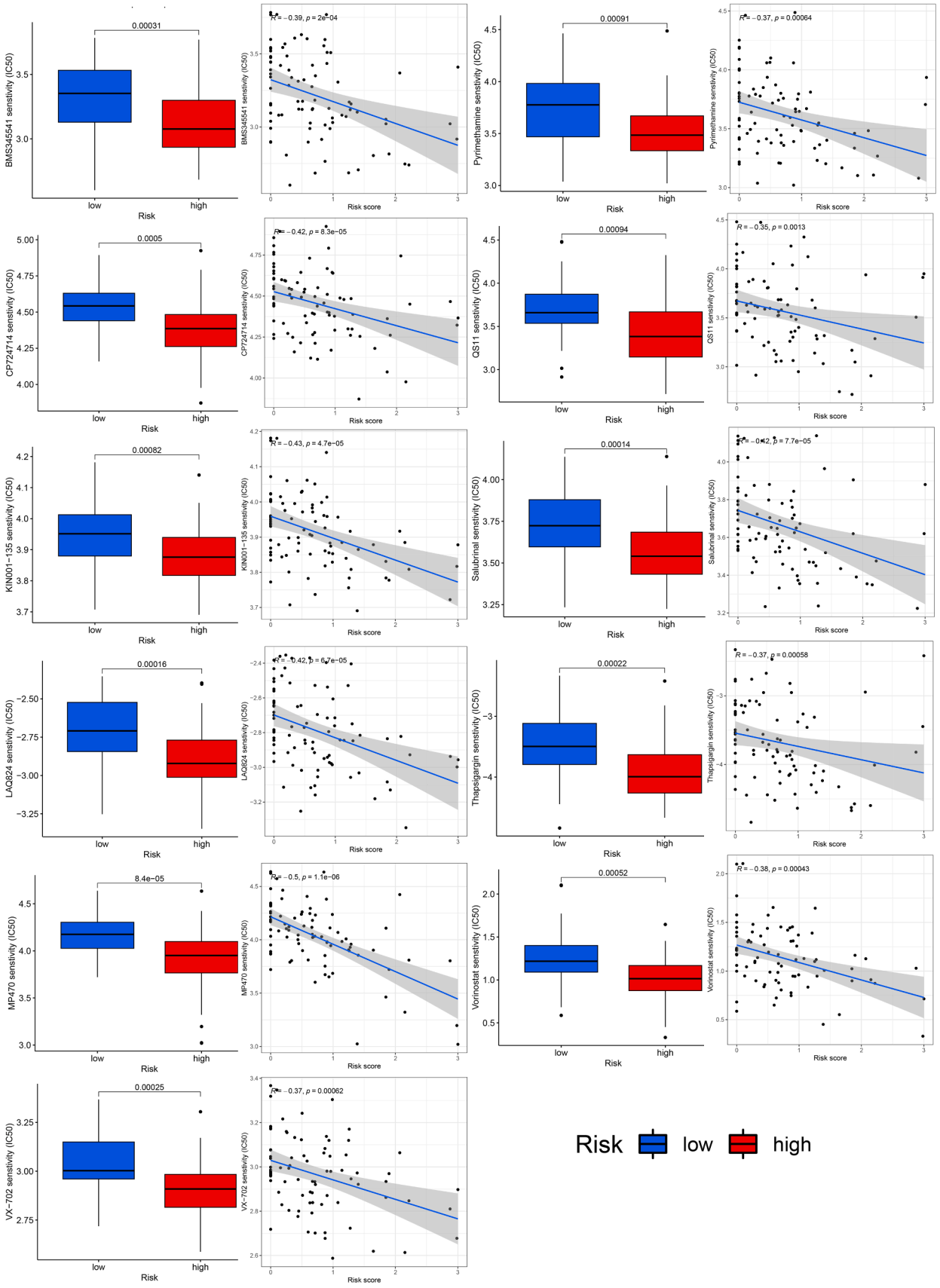

Fig. 14. Chemotherapeutic agent sensitivity analysis demonstrated that the RP11-472M19.2 high expression group was more sensitive to BMS345541, CP724714, and KIN001-135, etc.

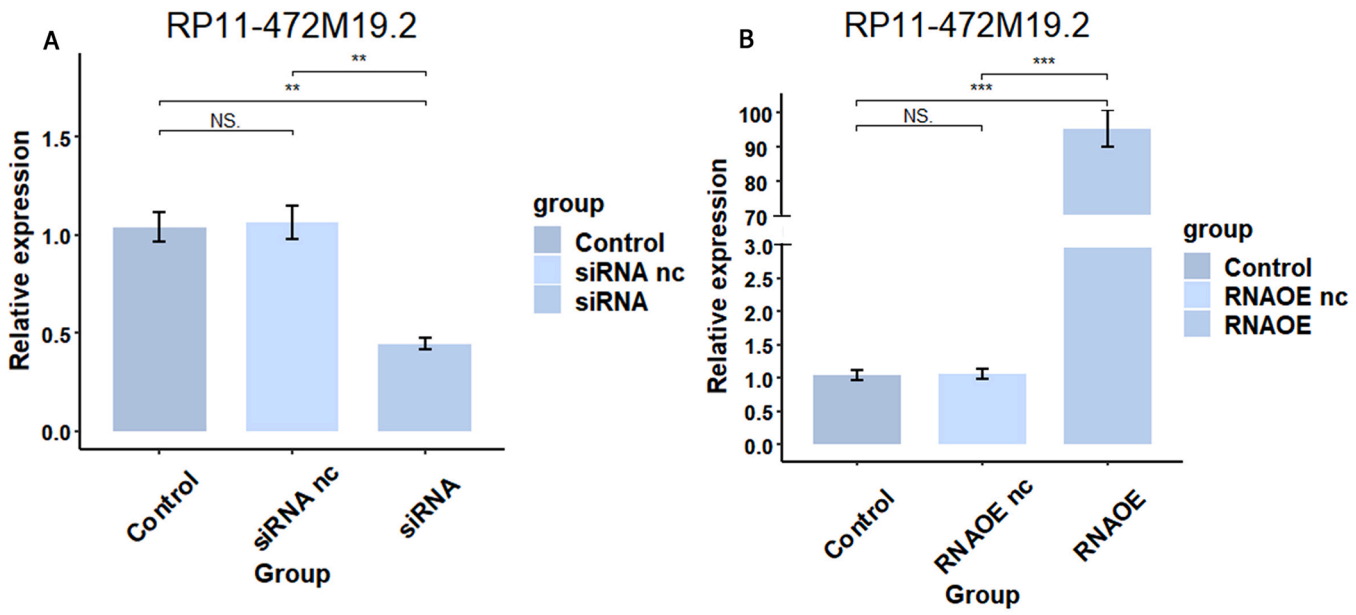

Fig. 15. Expression level of RP11-472M19.2 was successfully knocked down(A) or overexpressed(B) in Saos-2 cells verified by qRT-PCR.

metastasis using RP11-472M19.2 was up to 0.787. Further correlation analysis revealed that RP11-472M19.2 is positively correlated with genes such as MET, FASN, HES4, EZH2, DNMT3A, and HEY1 those promote osteosarcoma metastasis and negatively correlated with genes such as FAS and DCN that inhibit osteosarcoma metastasis [42–49], which suggests that RP11-472M19.2 may promote osteosarcoma metastasis. We further investigated RP11-472M19.2 by cell proliferation, migration, and invasion assay. EdU assay showed that RP11-472M19.2 significantly increased the proliferation ability of Saos-2 cells. In addition, wound healing assay confirmed that RP11-472M19.2 increased the migration ability of osteosarcoma cells. The invasion assay demonstrated that RP11-472M19.2 significantly enhanced the invasion ability of osteosarcoma cells. We screened the 100 genes most positively or negatively associated with RP11-472M19.2 for enrichment analysis and found that they were significantly enriched in protein digestion and absorption, proteoglycans in cancer, relaxin signaling pathway, integrin binding, extracellular matrix binding, external encapsulating structure organization, cell substrate adhesion, response to amino acid, cellular response to acid chemical, response to hyperoxia pathways. The differential expressed genes between the high and low RP11-472M19.2 expression subgroups were significantly enriched in acidic amino acid transport, amino acid transport, carboxylic acid transport, cell-cell contact zone, skeletal muscle organ development, which is in partial correspondence with the previous results, suggested that RP11-472M19.2 probably affects the progression of osteosarcoma through protein digestion and absorption, amino acid metabolism and intercellular contact regions, which also needs to be further explored in the future. The above results suggest that RP11-472M19.2 may be a valuable therapeutic target of osteosarcoma, providing novel ideas in the clinical management of osteosarcoma.

Numerous studies have previously demonstrated that lactate metabolism-associated lncRNAs significantly affect the evolution of various tumors. Li et al [32] successfully developed a lactate metabolism-associated lncRNAs signature for predicting the prognosis of breast cancer; Xia et al [50] developed a signature to assess the prognosis of patients with hepatocellular carcinoma using lactate metabolism-associated lncRNAs which was found to be significantly relevant to immune infiltration; Mai et al [51] generated a lactate metabolism-associated lncRNAs marker that accurately predicted lung cancer prognosis and had a significant impact on the tumor immune microenvironment. However, studies on genes related to lactate metabolism are still relatively scarce in the progression of osteosarcoma. Among the five lncRNAs related to osteosarcoma prognosis identified in this research, a previous study by Song et al [52] showed that FAM222A-AS1 promotes tumor growth as well as the proliferation and migration of colorectal cancer (CRC) cells; While Zhang et al [53] found that FAM222A-AS1 may be present as a protective factor in the metastasis and prognosis of lung adenocarcinoma (LUAD). However, there are no remaining lncRNAs-related studies, and this research establishes the association between these five lactate metabolism-associated lncRNAs and the progression of osteosarcoma for the first time.

Traditional chemotherapy in oncology treatment has limitations, and immunotherapy is now rapidly evolving and becoming an effective supplemental therapy [54], and numerous studies have confirmed that lactic acid suppresses the proliferation and activity of immune cells as well as facilitates tumor evasion of the immune response [55–58]. To explore the potential value of LRPS for the immunological therapy of osteosarcoma, we also conducted differential analyses of the immune microenvironment for different risk subgroups. The results demonstrated that both immune scores and ESTIMATE scores significantly decreased and the tumor purity significantly higher in the high-risk group. Immune cell analysis showed a significant decrease in various immune cells in the high-risk group, including B cells, CD8+ T cells, DCs, Neutrophils, T helper cells, Th2 cells, TIL, etc. Immune function analysis revealed that T cell co-stimulation score was significantly decreased in the high-risk group, and immune heat map revealed significant differences in the status of the immunological microenvironment between two risk subgroups, suggesting that patients of low-risk group have better immune infiltration and may respond to immunotherapy much more effectively [59,60]. Immune checkpoint analysis showed that LAG3 and LGALS9 expression levels were significantly higher in the low-risk group compared to the high-risk group, while CD160 and ICOSLG showed the opposite trend, and previous analyses have shown that the LAG3 checkpoint can serve as a valuable target for osteosarcoma treatment. [61], which suggests that the LAG3 checkpoint may be an effective potential target for osteosarcoma treatment. These demonstrate that LRPS could be a promising standard of immunotherapy for osteosarcoma patients. and that lactate metabolism-related lncRNAs may influence osteosarcoma progression by affecting the function and status of immune cells, which is consistent with previous studies [11,30,62-64]. Heuser et al [11] have shown that lactate metabolism can suppress antitumor immunity through inhibition of effector

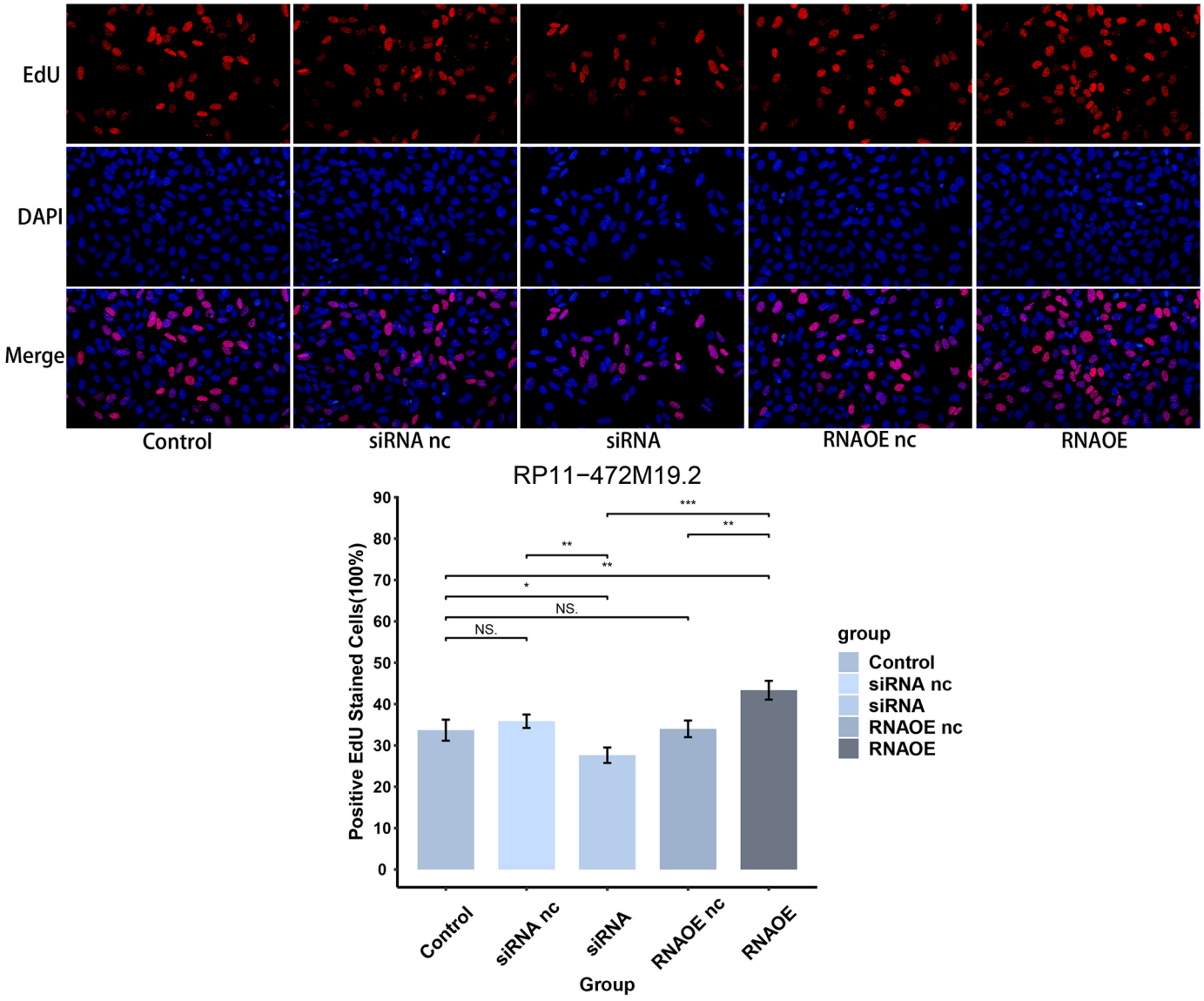

Fig. 16. Knockdown or overexpression of RP11-472M19.2 modulated the proliferation of Saos-2 cells accordingly.

immune cell populations; Whereas Xiao et al [30] showed that lactic acid metabolism in tumor microenvironment may influence the infiltration of immune cells and used lactate metabolism-associated lncRNAs to construct a prognostic signature that has strong prognostic potential for colon adenocarcinoma (COAD) and which correlates significantly with the immune profile of the tumor; Zheng et al [12] reduced intra-tumor lactate by mCuLP nanosystems, thereby improving the immunosuppressed tumor microenvironment and promoting tumor cell apoptosis; Zhu et al [65] constructed a lactate score to independently predict the prognosis of colorectal cancer and as an evaluation factor for the efficacy of immunotherapy. Moreover, our study demonstrates for the first time the influence of lactate metabolism-associated lncRNAs on the tumor microenvironment and immune infiltration in osteosarcoma, which has guiding implications for the immunotherapy of osteosarcoma. Wu et al. [66] selected fatty acid and lactate metabolism-related genes to construct a prognostic prediction model that also had a significant effect on the tumor immune microenvironment, which had similarities with our study, but it is worth discussing that our study focused on a finer perspective of lactate metabolism and limited to lncRNAs, a popular target for a variety of cancers, to construct a prognostic prediction model with higher diagnostic value. The AUC values for predicting 1-, 3-, and 5-year survival in osteosarcoma reached 0.943, 0.927, and 0.947, respectively, compared with only 0.841, 0.750, and 0.750, respectively, in the model of Wu et al. We constructed a nomogram with the equally promising predictive effect of Wu, but we also performed a cindex analysis on the nomogram, and the results demonstrated that Our nomogram had stronger stability and the ROC curve showed that nomo values could accurately predict survival in osteosarcoma patients at different periods (AUC values of 0.868, 0.867, and 0.839 at 1, 3, and 5 years). Clinical subgroup validation showed good applicability of LRPS. We analyzed each DELRRs of LRPS independently and found that more than half of the them could independently predicted patient survival and identified a potential role of RP11-472M19.2 for osteosarcoma metastasis, and the results were also well validated experimentally. We therefore believe that our study is a more uanced and deeper research based on that of Wu et al. and yielded results with greater predictive power and greater stability.

The IC50 of chemotherapeutic agents is generally used for indicating the sensitivity of tumors to chemotherapeutic agents. Numerous researchers have predicted the sensitivity of tumors to different drugs based on the IC50 to discover individualized treatment strategies for different tumor patients [67–70]. The results of our chemotherapeutic

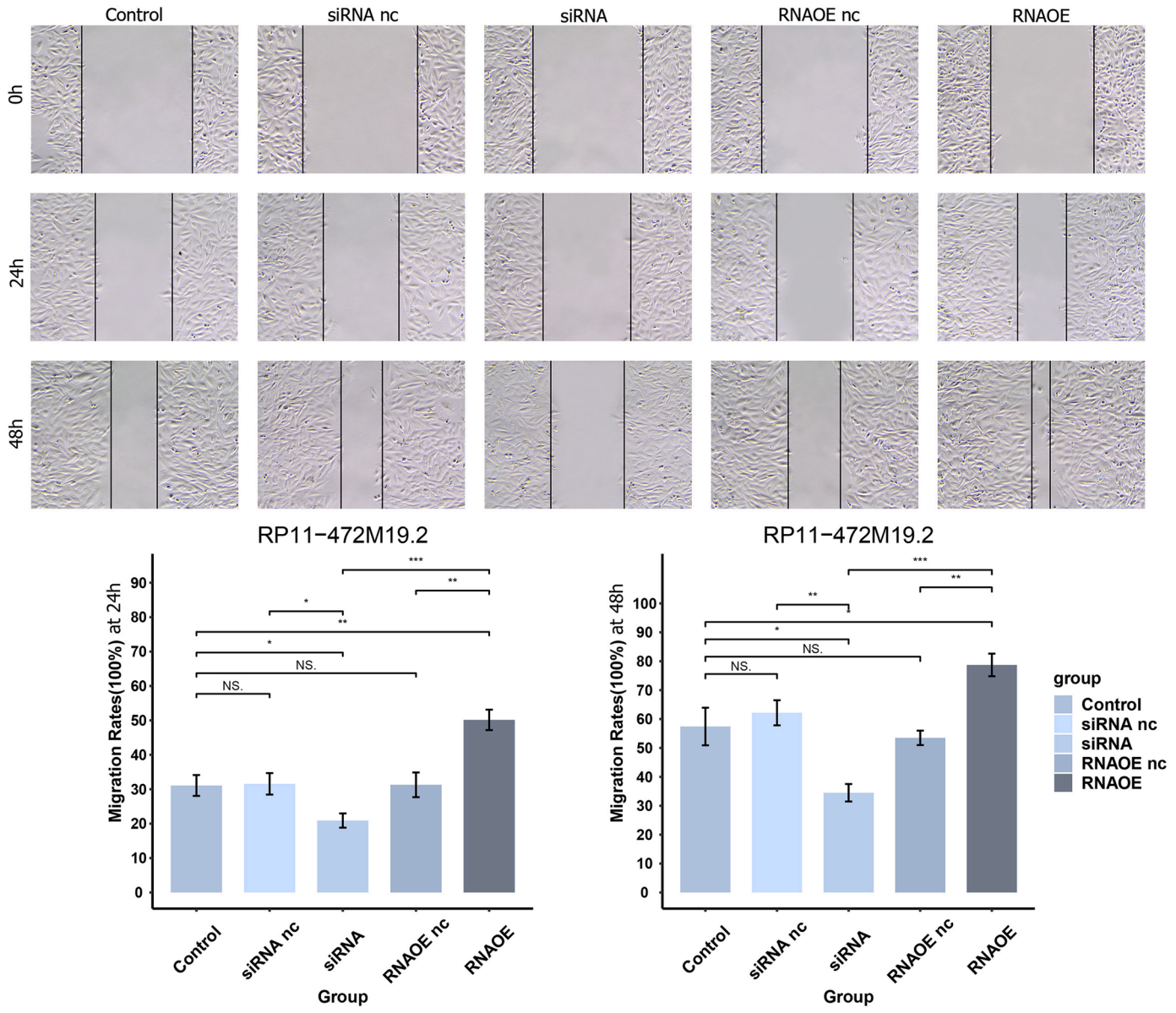

Fig. 17. Knockdown or overexpression of RP11-472M19.2 modulated the migration of Saos-2 cells accordingly.

agents sensitivity analysis indicated that patients of high-risk group have lower IC50 values for BMS345541 and JNK-9L, suggesting that these patients had greater sensitivity to both agents. And drug sensitivity analysis based on RP11-472M19.2 expression indicated that osteosarcoma patients with high RP11-472M19.2 expression may be more sensitive to BMS345541, CP724714, KIN001-135 and other drugs. Therefore, both our prognostic signature LRPS and RP11-472M19.2 can be used as promising guiding criteria for personalized chemotherapy of osteosarcoma patients and help to select the most appropriate chemotherapy protocol for osteosarcoma patients.

Lactate metabolism has been gradually demonstrated as a potential therapeutic target for various tumors, while lncRNAs influence tumor progression through various biological pathways. Our research presents a novel insight into the progression and management of osteosarcoma from the perspective of lactate metabolism, exploring the link between lactate metabolism, lncRNA, and osteosarcoma, and offer innovative ideas for osteosarcoma therapy.

We have reviewed major databases including GEO without finding a dataset containing expression matrices for the 5 DELRLs and clinical information, so there is a limitation in our sample size to externally validate the constructed signature to improve its applicability, so further preclinical experiments are needed to validate our conclusions. We have not performed in vitro experiments to verify that RP11-472M19.2 affects osteosarcoma metastasis due to conditions. An increasing number of studies have shown complex interactions and potential crosstalk between lncRNAs and microRNAs and mRNAs, but we focused our study on lncRNAs and did not explore microRNAs and mRNAs in depth, which became a limitation of this study, and the future impact of microRNAs and miRNAs on the prognosis of osteosarcoma deserves further exploration [71,72]. Overall, this prognostic feature has a high prognostic predictive value for osteosarcoma and its value in immune microenvironment and personalized therapeutic instruction has been fully explored, and the effect of RP11-472M19.2 gene on the progression of osteosarcoma has been experimentally validated. Meanwhile, we plan to collect more clinical samples for further validation of the signature.

Conclusion

This research illustrates the effect of lactate metabolism associated lncRNAs on osteosarcoma progression and potential mechanisms for the

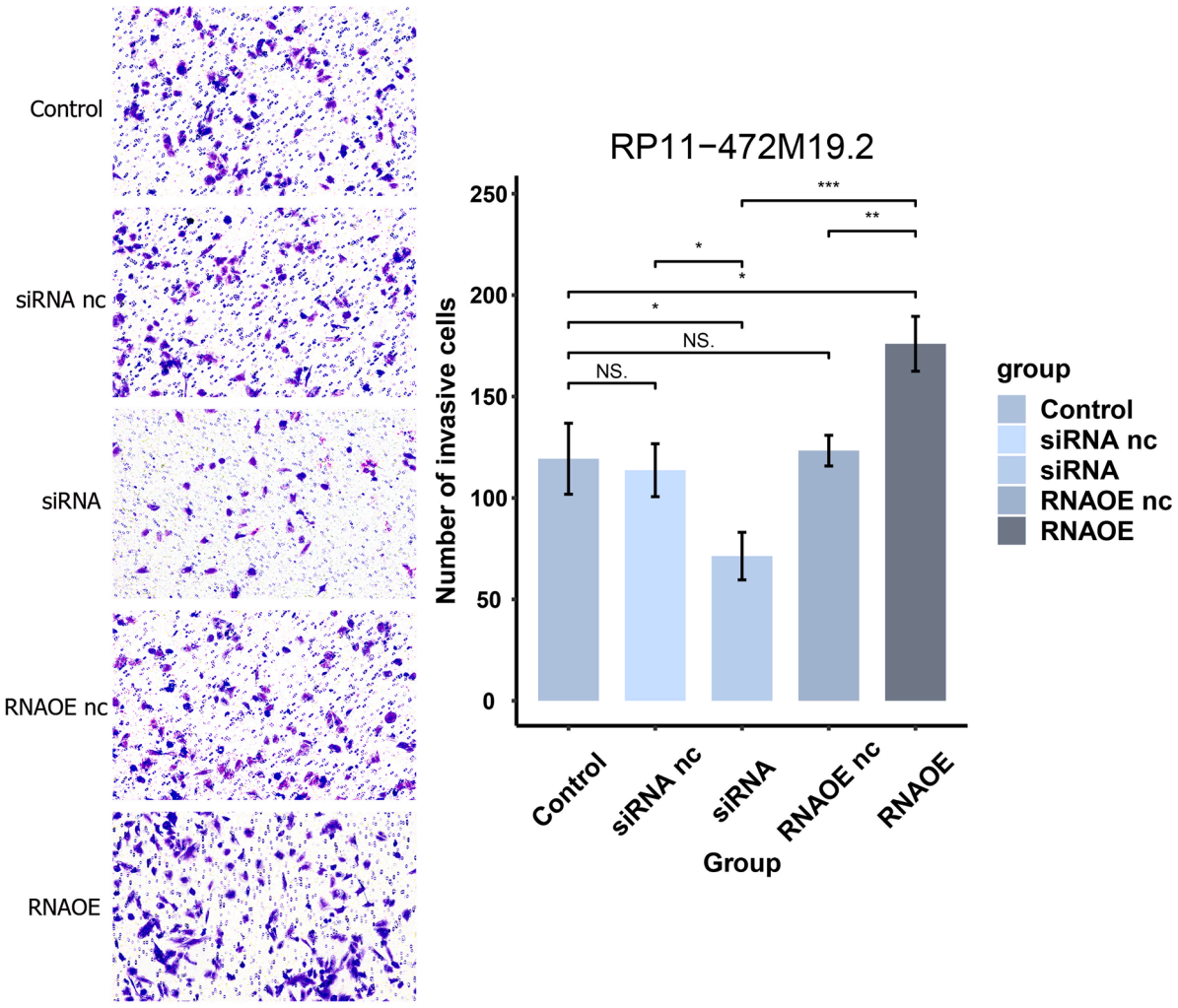

Fig. 18. Knockdown or overexpression of RP11-472M19.2 modulated the invasion of Saos-2 cells accordingly.

first time, tapped the potential role of RP11-472M19.2 in osteosarcoma, and was validated by adequate experiments, our discoveries are instructive for the clinical management and deeper study of osteosarcoma.

CRediT authorship contribution statement

Liangkun Huang: Conceptualization, Software, Validation, Investigation, Writing – review & editing. **Xiaoshuang Zeng:** Conceptualization, Writing – original draft. **Wanting Liang:** Data curation. **Junwen Chen:** Software. **Changheng Zhong:** Validation. **Wenxiang Cai:** Validation. **Xuezhong Wang:** Formal analysis. **Zhengjie Zhu:** Resources. **Li Su:** Methodology. **Zilin Liu:** Visualization. **Hao Peng:** Visualization, Project administration, Funding acquisition.

Declaration of Competing Interest

All authors declare that we do not have any commercial or associative interest that represents a conflict of interest in connection with the work submitted.

Funding

This research was funded by the National Natural Science Foundation of China (grant number 81672154).

References

[1] HC Beird, SS Bielack, AM Flanagan, J Gill, D Heymann, KA Janeway, JA Livingston, RD Roberts, SJ Strauss, R Gorlick, Osteosarcoma, Nat Rev Dis Primers 8 (1) (2022) 77.
[2] H Wang, X Zhou, C Li, S Yan, C Feng, J He, Z Li, C Tu, The emerging role of pyroptosis in pediatric cancers: from mechanism to therapy, J Hematol Oncol 15 (1) (2022) 140.
[3] Y Liu, G Qiu, Y Luo, S Li, Y Xu, Y Zhang, J Hu, P Li, H Pan, Y Wang, Circular RNA ROCK1, a novel circRNA, suppresses osteosarcoma proliferation and migration via altering the miR-532-5p/PTEN axis, Exp Mol Med 54 (7) (2022) 1024–1037.
[4] C Zeng, L Zhong, W Liu, Y Zhang, X Yu, X Wang, R Zhang, T Kang, D Liao, Targeting the Lysosomal Degradation of Rab22a-NeoF1 Fusion Protein for Osteosarcoma Lung Metastasis, Adv Sci (Weinh) 10 (5) (2023), e2205483.
[5] L Yu, J Zhang, Y Li, Effects of microenvironment in osteosarcoma on chemoresistance and the promise of immunotherapy as an osteosarcoma therapeutic modality, Front Immunol 13 (2022), 871076.
[6] E Baidya Kayal, S Bakhshi, D Kandasamy, MC Sharma, SA Khan, VS Kumar, K Khare, R Sharma, A Mehndiratta, Non-invasive intravoxel incoherent motion MRI in prediction of histopathological response to neoadjuvant chemotherapy and survival outcome in osteosarcoma at the time of diagnosis, J Transl Med 20 (1) (2022) 625.
[7] W-B Liu, S-H Dong, W-H Hu, M Gao, T Li, Q-B Ji, X-Q Yang, D-B Qi, Z Zhang, Z-L Song, et al., A simple, universal and multifunctional template agent for personalized treatment of bone tumors, Bioact Mater 12 (2022) 292–302.
[8] Y Fu, G He, Z Liu, J Wang, M Li, Z Zhang, Q Bao, J Wen, X Zhu, C Zhang, et al., DNA Base Pairing-Inspired Supramolecular Nanodrug Camouflaged by Cancer-Cell Membrane for Osteosarcoma Treatment, Small 18 (30) (2022), e2202337.
[9] X Li, Y Yang, B Zhang, X Lin, X Fu, Y An, Y Zou, J-X Wang, Z Wang, T Yu, Lactate metabolism in human health and disease, Signal Transduct Target Ther 7 (1) (2022) 305.
[10] P Apostolova, EL Pearce, Lactic acid and lactate: revisiting the physiological roles in the tumor microenvironment, Trends Immunol 43 (12) (2022) 969–977.

[11] C Heuser, K Renner, M Kreutz, L Gattinoni, Targeting lactate metabolism for cancer immunotherapy - a matter of precision, Semin Cancer Biol 88 (2023) 32–45.
[12] X Zheng, Y Liu, Y Liu, T Zhang, Y Zhao, J Zang, Y Yang, R He, G Chong, S Ruan, et al., Dual Closed-Loop of Catalyzed Lactate Depletion and Immune Response to Potentiate Photothermal Immunotherapy, ACS Appl Mater Interfaces (2022).
[13] C Hayes, CL Donohoe, M Davern, NE Donlon, The oncogenic and clinical implications of lactate induced immunosuppression in the tumour microenvironment, Cancer Lett 500 (2021) 75–86.
[14] Q Xiao, Z Wei, Y Li, X Zhou, J Chen, T Wang, G Shao, M Zhang, Z Zhang, miR-186 functions as a tumor suppressor in osteosarcoma cells by suppressing the malignant phenotype and aerobic glycolysis, Oncol Rep 39 (6) (2018) 2703–2710.
[15] X Han, Y Yang, Y Sun, L Qin, Y Yang, LncRNA TUG1 affects cell viability by regulating glycolysis in osteosarcoma cells, Gene 674 (2018) 87–92.
[16] B Yu, F Zhang, L Liu, Y Liang, X Tang, Y Peng, F Cai, D Zeng, X Yuan, J Li, et al., The novel prognostic risk factor STC2 can regulate the occurrence and progression of osteosarcoma via the glycolytic pathway, Biochem Biophys Res Commun 554 (2021) 25–32.
[17] Z Li, M Geng, X Ye, Y Ji, Y Li, X Zhang, W Xu, IRF7 inhibits the Warburg effect via transcriptional suppression of PKM2 in osteosarcoma, Int J Biol Sci 18 (1) (2022) 30–42.
[18] F Ling, Q Lu, S100 calcium-binding protein A10 contributes to malignant traits in osteosarcoma cells by regulating glycolytic metabolism via the AKT/mTOR pathway, Bioengineered 13 (5) (2022) 12298–12308.
[19] Q Wang, M-J Liu, J Bu, J-L Deng, B-Y Jiang, L-D Jiang, X-J He, miR-485-3p regulated by MALAT1 inhibits osteosarcoma glycolysis and metastasis by directly suppressing c-MET and AKT3/mTOR signalling, Life Sci 268 (2021), 118925.
[20] M Hashemi, MS Moosavi, HM Abed, M Dehghani, M Aalipour, EA Heydari, M Behroozaghdam, M Entezari, S Salimimoghadam, ES Gunduz, et al., Long non-coding RNA (lncRNA) H19 in human cancer: From proliferation and metastasis to therapy, Pharmacol Res 184 (2022), 106418.
[21] J Yan, R Wang, J Tan, Recent advances in predicting lncRNA-disease associations based on computational methods, Drug Discov Today 28 (2) (2023), 103432.
[22] Y Zhang, X Dong, X Guo, C Li, Y Fan, P Liu, D Yuan, X Ma, J Wang, J Zheng, et al., LncRNA-BC069792 suppresses tumor progression by targeting KCNQ4 in breast cancer, Mol Cancer 22 (1) (2023) 41.
[23] Y-L Liang, Y Zhang, X-R Tan, H Qiao, S-R Liu, L-L Tang, Y-P Mao, L Chen, W-F Li, G-Q Zhou, et al., A lncRNA signature associated with tumor immune heterogeneity predicts distant metastasis in locoregionally advanced nasopharyngeal carcinoma, Nat Commun 13 (1) (2022) 2996.
[24] Y Liu, M Shi, X He, Y Cao, P Liu, F Li, S Zou, C Wen, Q Zhan, Z Xu, et al., LncRNA-PACERR induces pro-tumour macrophages via interacting with miR-671-3p and m6A-reader IGF2BP2 in pancreatic ductal adenocarcinoma, J Hematol Oncol 15 (1) (2022) 52.
[25] Q Wu, H Zhang, D Yang, Q Min, Y Wang, W Zhang, Q Zhan, The m6A-induced lncRNA CASC8 promotes proliferation and chemoresistance via upregulation of hnRNPL in esophageal squamous cell carcinoma, Int J Biol Sci 18 (13) (2022) 4824–4836.
[26] Z Cheng, C Lu, H Wang, N Wang, S Cui, C Yu, C Wang, Q Zuo, S Wang, Y Lv, et al., Long noncoding RNA LHFPL3-AS2 suppresses metastasis of non-small cell lung cancer by interacting with SFPQ to regulate TXNIP expression, Cancer Lett (2022) 531.
[27] R Kufukihara, N Tanaka, K Takamatsu, N Niwa, K Fukumoto, Y Yasumizu, T Takeda, K Matsumoto, S Morita, T Kosaka, et al., Hybridisation chain reaction-based visualisation and screening for lncRNA profiles in clear-cell renal-cell carcinoma, Br J Cancer 127 (6) (2022) 1133–1141.
[28] Y Wang, S Zheng, J Han, N Li, R Ji, X Li, C Han, W Zhao, L Zhang, LINC00629 protects osteosarcoma cell from ER stress-induced apoptosis and facilitates tumour progression by elevating KLF4 stability, J Exp Clin Cancer Res 41 (1) (2022) 354.
[29] M Yang, H Zheng, K Xu, Q Yuan, Y Aihaiti, Y Cai, P Xu, A novel signature to guide osteosarcoma prognosis and immune microenvironment: Cuproptosis-related lncRNA, Front Immunol 13 (2022), 919231.
[30] J Xiao, X Wang, Y Liu, X Liu, J Yi, J Hu, Lactate Metabolism-Associated lncRNA Pairs: A Prognostic Signature to Reveal the Immunological Landscape and Mediate Therapeutic Response in Patients With Colon Adenocarcinoma, Front Immunol 13 (2022), 881359.
[31] J Han, X Chen, J Wang, B Liu, Glycolysis-related lncRNA TMEM105 upregulates LDHA to facilitate breast cancer liver metastasis via sponging miR-1208, Cell Death Dis 14 (2) (2023) 80.
[32] J Li, Y Zhang, C Li, H Wu, C Feng, W Wang, X Liu, Y Zhang, Y Cai, Y Jia, et al., A lactate-related LncRNA model for predicting prognosis, immune landscape and therapeutic response in breast cancer, Front Genet 13 (2022), 956246.
[33] F Liu, Z Dai, Q Cheng, L Xu, L Huang, Z Liu, X Li, N Wang, G Wang, L Wang, et al., LncRNA-targeting bio-scaffold mediates triple immune effects for postoperative colorectal cancer immunotherapy, Biomaterials 284 (2022), 121485.
[34] Y Bai, Q Zhang, F Liu, J Quan, A novel cuproptosis-related lncRNA signature predicts the prognosis and immune landscape in bladder cancer, Front Immunol 13 (2022), 1027449.
[35] X Li, Z Zhang, M Liu, X Fu, J A, G Chen, S Wu, J-T Dong, Establishment of a lncRNA-Based Prognostic Gene Signature Associated With Altered Immune Responses in HCC, Front Immunol 13 (2022), 880288.
[36] W Zhang, Z Liu, J Wang, B Geng, W Hou, E Zhao, X Li, The clinical significance, immune infiltration, and tumor mutational burden of angiogenesis-associated lncRNAs in kidney renal clear cell carcinoma, Front Immunol 13 (2022), 934387.
[37] L Luan, Y Dai, T Shen, C Yang, Z Chen, S Liu, J Jia, Z Li, S Fang, H Qiu, et al., Development of a novel hypoxia-immune-related LncRNA risk signature for predicting the prognosis and immunotherapy response of colorectal cancer, Front Immunol 13 (2022), 951455.
[38] H Li, Z-Y Liu, Y-C Chen, X-Y Zhang, N Wu, J Wang, Identification and validation of an immune-related lncRNAs signature to predict the overall survival of ovarian cancer, Front Oncol 12 (2022), 999654.
[39] J Yao, X Chen, X Liu, R Li, X Zhou, Y Qu, Characterization of a ferroptosis and iron-metabolism related lncRNA signature in lung adenocarcinoma, Cancer Cell Int 21 (1) (2021) 340.
[40] X Wang, C Dai, M Ye, J Wang, W Lin, R Li, Prognostic value of an autophagy-related long-noncoding-RNA signature for endometrial cancer, Aging (Albany NY) 13 (4) (2021) 5104–5119.
[41] K Zhang, L Ping, T Du, G Liang, Y Huang, Z Li, R Deng, J Tang, A Ferroptosis-Related lncRNAs Signature Predicts Prognosis and Immune Microenvironment for Breast Cancer, Front Mol Biosci 8 (2021), 678877.
[42] G Wang, M Sun, Y Jiang, T Zhang, W Sun, H Wang, F Yin, Z Wang, W Sang, J Xu, et al., Anlotinib, a novel small molecular tyrosine kinase inhibitor, suppresses growth and metastasis via dual blockade of VEGFR2 and MET in osteosarcoma, Int J Cancer 145 (4) (2019) 979–993.
[43] T Sun, X Zhong, H Song, J Liu, J Li, F Leung, WW Lu, Z-L Liu, Anoikis resistant mediated by FASN promoted growth and metastasis of osteosarcoma, Cell Death Dis 10 (4) (2019) 298.
[44] M McManus, E Kleinerman, Y Yang, JA Livingston, J Mortus, R Rivera, P Zweidler-McKay, K Schadler, Hes4: A potential prognostic biomarker for newly diagnosed patients with high-grade osteosarcoma, Pediatr Blood Cancer 64 (5) (2017).
[45] C-Y Xing, Y-Z Zhang, W Hu, L-Y Zhao, LINC00313 facilitates osteosarcoma carcinogenesis and metastasis through enhancing EZH2 mRNA stability and EZH2-mediated silence of PTEN expression, Cell Mol Life Sci 79 (7) (2022) 382.
[46] X Tan, C Zeng, H Li, Y Tan, H Zhu, Circ0038632 modulates MiR-186/DNMT3A axis to promote proliferation and metastasis in osteosarcoma, Front Oncol 12 (2022), 939994.
[47] A Tsuru, T Setoguchi, Y Matsunoshita, H Nagao-Kitamoto, S Nagano, M Yokouchi, S Maeda, Y Ishidou, T Yamamoto, S Komiya, Hairy/enhancer-of-split related with YRPW motif protein 1 promotes osteosarcoma metastasis via matrix metallopeptidase 9 expression, Br J Cancer 112 (7) (2015) 1232–1240.
[48] Y Yang, G Huang, Z Zhou, JG Fewell, Kleinerman ES: miR-20a Regulates FAS Expression in Osteosarcoma Cells by Modulating FAS Promoter Activity and Can be Therapeutically Targeted to Inhibit Lung Metastases, Mol Cancer Ther 17 (1) (2018) 130–139.
[49] D Xiao, Y Lu, L Zhu, T Liang, Z Wang, J Ren, R He, K Wang, Anti-osteosarcoma property of decorin-modified titanium surface: A novel strategy to inhibit oncogenic potential of osteosarcoma cells, Biomed Pharmacother 125 (2020), 110034.
[50] X Xia, H Zhang, P Xia, Y Zhu, J Liu, K Xu, Y Yuan, Identification of Glycolysis-Related lncRNAs and the Novel lncRNA WAC-AS1 Promotes Glycolysis and Tumor Progression in Hepatocellular Carcinoma, Front Oncol 11 (2021), 733595.
[51] S Mai, L Liang, G Mai, X Liu, D Diao, R Cai, L Liu, Development and Validation of Lactate Metabolism-Related lncRNA Signature as a Prognostic Model for Lung Adenocarcinoma, Front Endocrinol (Lausanne) 13 (2022), 829175.
[52] M Song, Y Li, Z Chen, J Zhang, L Yang, F Zhang, C Song, M Miao, W Chang, H Shi, The Long Non-Coding RNA FAM222A-AS1 Negatively Modulates MiR-Let-7f to Promote Colorectal Cancer Progression, Front Oncol 12 (2022), 764621.
[53] X Zhang, J Han, L Du, X Li, J Hao, L Wang, G Zheng, W Duan, Y Xie, Y Zhao, et al., Unique metastasis-associated lncRNA signature optimizes prediction of tumor relapse in lung adenocarcinoma, Thorac Cancer 11 (3) (2020) 728–737.
[54] H Tian, J Cao, B Li, EC Nice, H Mao, Y Zhang, C Huang, Managing the immune microenvironment of osteosarcoma: the outlook for osteosarcoma treatment, Bone Res 11 (1) (2023) 11.
[55] Z Li, Q Wang, X Huang, M Yang, S Zhou, Z Li, Z Fang, Y Tang, Q Chen, H Hou, et al., Lactate in the tumor microenvironment: A rising star for targeted tumor therapy, Front Nutr 10 (2023), 1113739.
[56] L Kooshki, P Mahdavi, S Fakhri, EK Akkol, H Khan, Targeting lactate metabolism and glycolytic pathways in the tumor microenvironment by natural products: A promising strategy in combating cancer, Biofactors 48 (2) (2022) 359–383.
[57] C Wang, Z Qu, L Chen, Y Pan, Y Tang, G Hu, R Gao, R Niu, Q Liu, X Gao, et al., Characterization of Lactate Metabolism Score in Breast and Thyroid Cancers to Assist Immunotherapy via Large-Scale Transcriptomic Data Analysis, Front Pharmacol 13 (2022), 928419.
[58] C Wang, T Lu, R Xu, S Luo, J Zhao, L Zhang, Multi-omics analysis to identify lung squamous carcinoma lactate metabolism-related subtypes and establish related index to predict prognosis and guide immunotherapy, Comput Struct Biotechnol J 20 (2022) 4756–4770.
[59] J Wu, Z Jin, J Lin, Y Fu, J Wang, Y Shen, Vessel state and immune infiltration of the angiogenesis subgroup and construction of a prediction model in osteosarcoma, Front Immunol 13 (2022), 992266.
[60] AR Cillo, E Mukherjee, NG Bailey, S Onkar, J Daley, C Salgado, X Li, D Liu, S Ranganathan, M Burgess, et al., Ewing Sarcoma and Osteosarcoma Have Distinct Immune Signatures and Intercellular Communication Networks, Clin Cancer Res 28 (22) (2022) 4968–4982.
[61] X Bu, J Liu, R Ding, Z Li, Prognostic Value of a Pyroptosis-Related Long Noncoding RNA Signature Associated with Osteosarcoma Microenvironment, J Oncol 2021 (2021), 2182761.
[62] J Li, H Qiao, F Wu, S Sun, C Feng, C Li, W Yan, W Lv, H Wu, M Liu, et al., A novel hypoxia- and lactate metabolism-related signature to predict prognosis and immunotherapy responses for breast cancer by integrating machine learning and bioinformatic analyses, Front Immunol 13 (2022), 998140.

[63] Z Jiang, Y Luo, L Zhang, H Li, C Pan, H Yang, T Cheng, J Chen, A Novel Risk Score Model of Lactate Metabolism for Predicting over Survival and Immune Signature in Lung Adenocarcinoma, Cancers (Basel) (15) (2022) 14.
[64] L Chen, L Huang, Y Gu, W Cang, P Sun, Y Xiang, Lactate-Lactylation Hands between Metabolic Reprogramming and Immunosuppression, Int J Mol Sci 23 (19) (2022).
[65] D Zhu, Y Jiang, H Cao, J Yang, Y Shu, H Feng, X Yang, X Sun, M Shao, Lactate: A regulator of immune microenvironment and a clinical prognosis indicator in colorectal cancer, Front Immunol 13 (2022), 876195.
[66] Z Wu, T Han, H Su, J Xuan, X Wang, Comprehensive analysis of fatty acid and lactate metabolism-related genes for prognosis value, immune infiltration, and therapy in osteosarcoma patients, Front Oncol 12 (2022), 934080.
[67] ME van Linde, M Labots, CG Brahm, KE Hovinga, PC De Witt Hamer, RJ Honeywell, R de Goeij-de Haas, AA Henneman, JC Knol, GJ Peters, et al., Tumor Drug Concentration and Phosphoproteomic Profiles After Two Weeks of Treatment With Sunitinib in Patients with Newly Diagnosed Glioblastoma, Clin Cancer Res 28 (8) (2022) 1595–1602.
[68] Y Shi, Q Zhang, M Zhang, Y Chen, J Sun, L Chen, S Liu, Z Liu, J Yang, C Wu, et al., Discovery of Dual Lysine Methyltransferase G9a and EZH2 Inhibitors with In Vivo Efficacy against Malignant Rhabdoid Tumor, J Med Chem (2023).
[69] N Wei, G Chao-Yang, Z Wen-Ming, L Ze-Yuan, S Yong-Qiang, Z Shun-Bai, Z Kai, M Yan-Chao, Z Hai-Hong, A ubiquitin-related gene signature for predicting prognosis and constructing molecular subtypes in osteosarcoma, Front Pharmacol 13 (2022), 904448.
[70] W Wang, Z Lu, M Wang, Z Liu, B Wu, C Yang, H Huan, P Gong, The cuproptosis-related signature associated with the tumor environment and prognosis of patients with glioma, Front Immunol 13 (2022), 998236.
[71] J-Y Wang, Y Yang, Y Ma, F Wang, A Xue, J Zhu, H Yang, Q Chen, M Chen, L Ye, et al., Potential regulatory role of lncRNA-miRNA-mRNA axis in osteosarcoma, Biomed Pharmacother 121 (2020), 109627.
[72] C-N Fan, L Ma, N Liu, Systematic analysis of lncRNA-miRNA-mRNA competing endogenous RNA network identifies four-lncRNA signature as a prognostic biomarker for breast cancer, J Transl Med 16 (1) (2018) 264.